

Supporting Information

Hollow, mesoporous, eutectic $Zn_{1-x}Mg_xO$ nano-spheres as solid acid-base catalysts for the highly regio-selective O-methylation of 1, 2-diphenols

Xuri Wang,^a Jianing Zhang,^a Guangxin Xie,^b Zuyong Yin,^a Jie Liu,^a and Xuebing Ma^{a,*}

^a College of Chemistry and Chemical Engineering, Southwest University, Chongqing, 400715, P. R. China

^b School of Science, Chongqing University of Posts and Telecommunications, Chongqing, 400065, P. R. China

* Corresponding author's email: zcyj123@swu.edu.cn

Table of contents

1. Image and particle size distribution of carbon sphere.....	S2.
2. Adsorption of Zn ²⁺ /Mg ²⁺ ions on carbon spheres.....	S2-4
3. Characterization of acid-base catalysts.....	S4-12
(1) Morphology	
(2) Structure	
(3) Textural property	
(4) Amount and strength of basic/acidic sites	
(5) Type of acid sites (Lewis or Brønsted)	
4. Regio-selective O-methylation	S13-18
(1) Optimization of reaction conditions	
(2) Catalytic performances of various acid-base catalysts	
(3) Reaction kinetics	
(4) Substrate scope	
(5) Reusability of catalyst	
5. Activation model of ZnO HMNSs and MgO HMNSs.....	S19
6. ¹ H NMR spectra of products.....	S20-29
7. GC spectra for the alkylations of various diphenols.....	S30-34

1. Image and particle size distribution of carbon sphere

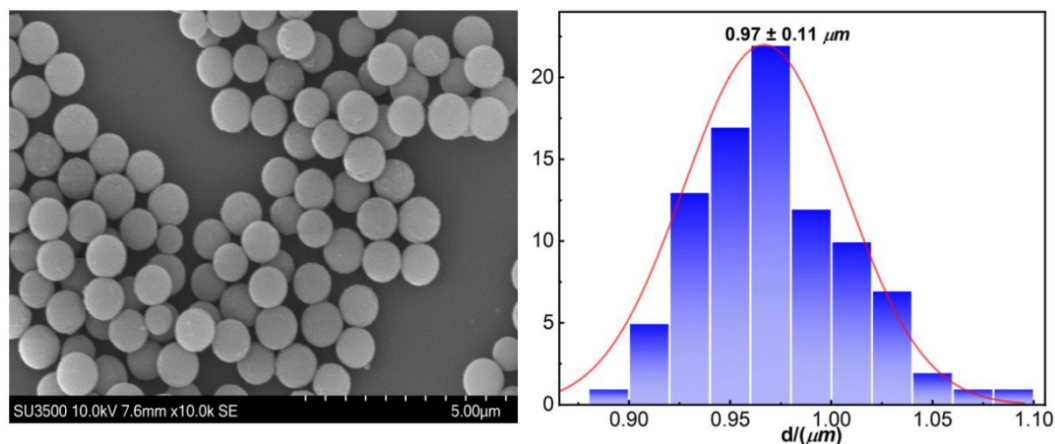


Fig. S1 SEM image and particle size distribution of carbon spheres.

2. Adsorption of Zn^{2+}/Mg^{2+} ions on carbon spheres

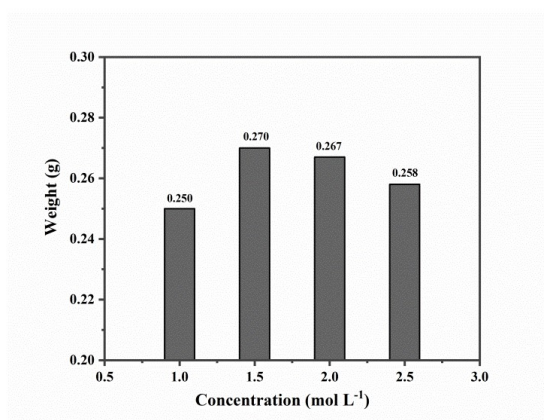


Fig. S2 Loading capacities of $Mg(NO_3)_2/Zn(NO_3)_2$ into carbon spheres (0.20 g) in aqueous mixed salt solutions (molar $Mg/Zn = 5/1$, 250 mL) with different concentrations at $160^\circ C$ for 6 h.

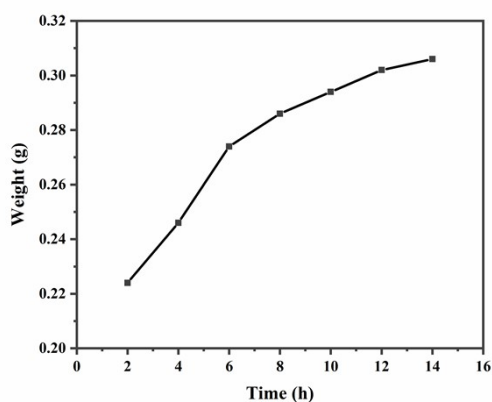


Fig. S3 Loading capacities of $Mg(NO_3)_2/Zn(NO_3)_2$ into carbon spheres (0.20 g) during 14 h (molar $Mg/Zn = 5/1$, $160^\circ C$, 250 mL of salt solution with $1.5 mol L^{-1}$).

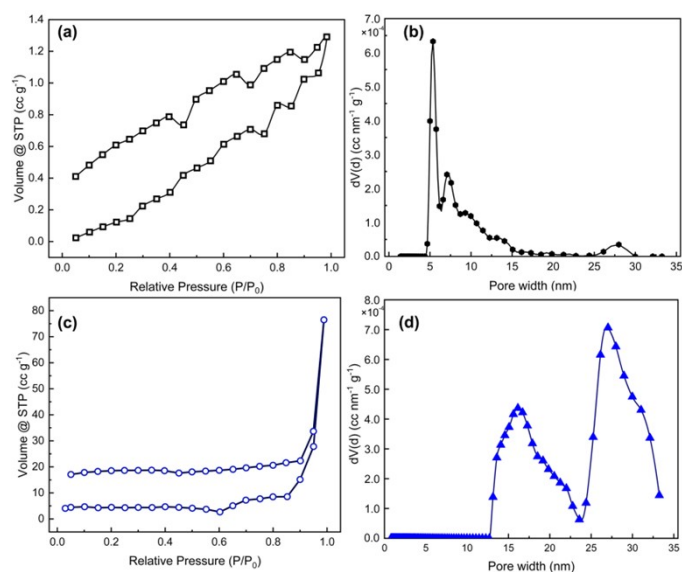


Fig. S4 N₂ adsorption-desorption isotherms (a, c) and pore size distributions (b, d) of carbon spheres before (a, b) and after (c, d) the adsorption of Mg²⁺ and Zn²⁺ ions.

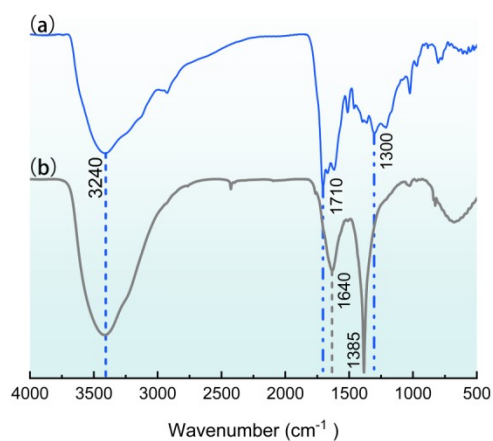


Fig. S5 IR spectra of carbon spheres after (a) and before (b) the adsorption of Mg²⁺ and Zn²⁺ ions.

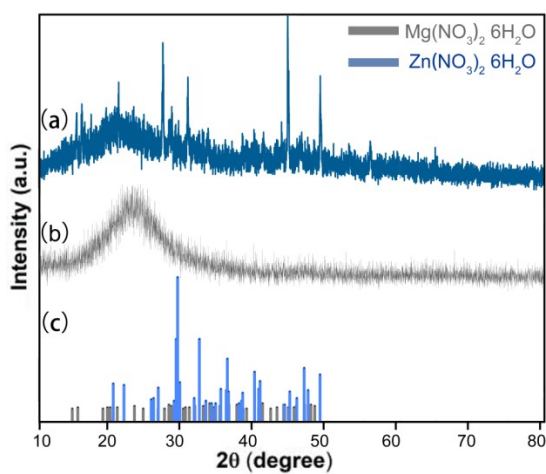


Fig S6 XRD pattern of Mg²⁺/Zn²⁺ ions-adsorbed carbon spheres (a), carbon spheres (b) and standard spectrum of Mg(NO₃)₂ and Zn(NO₃)₂ (c).

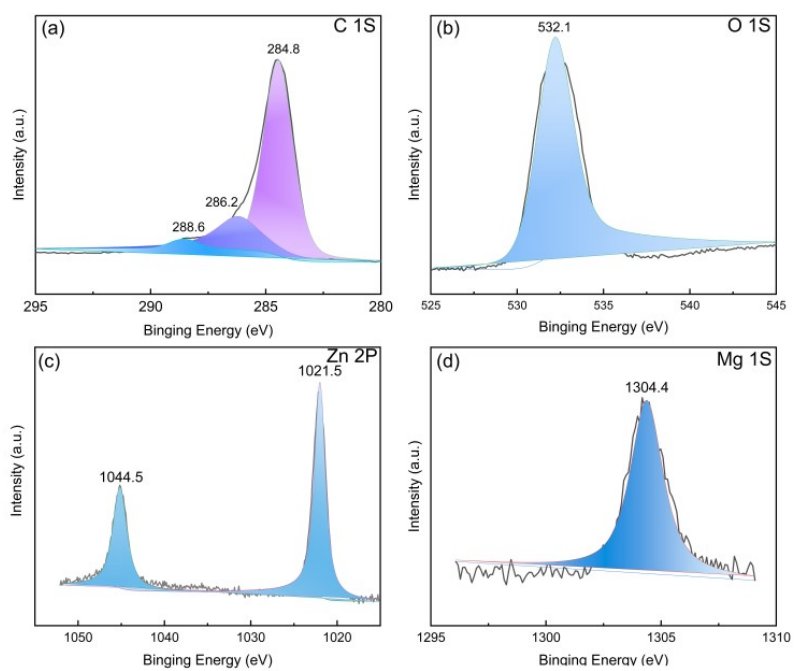


Fig. S7 XPS spectra of carbon spheres after the adsorption of Mg^{2+} and Zn^{2+} ions: C 1s (a), O 1s (b), Zn 2p (c), and Mg 1s (d).

3. Characterization of acid-base catalysts

(1) Morphology

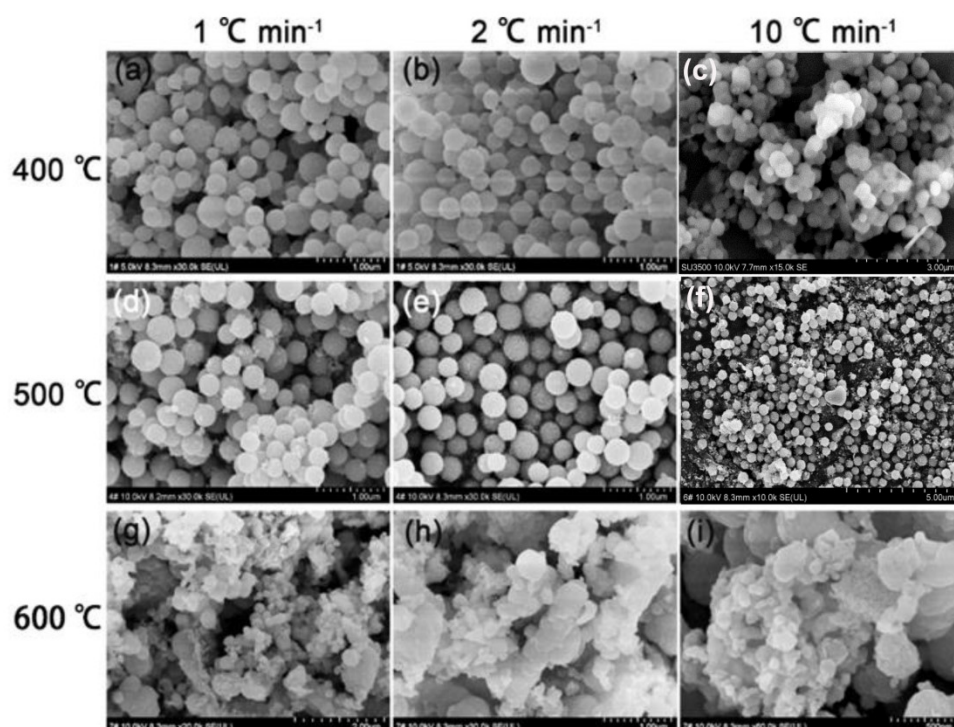


Fig. S8 Morphology of $Zn_{1-x}Mg_xO$ HMNSs ($x = 0.052$) under different calcination temperatures and heating rates.

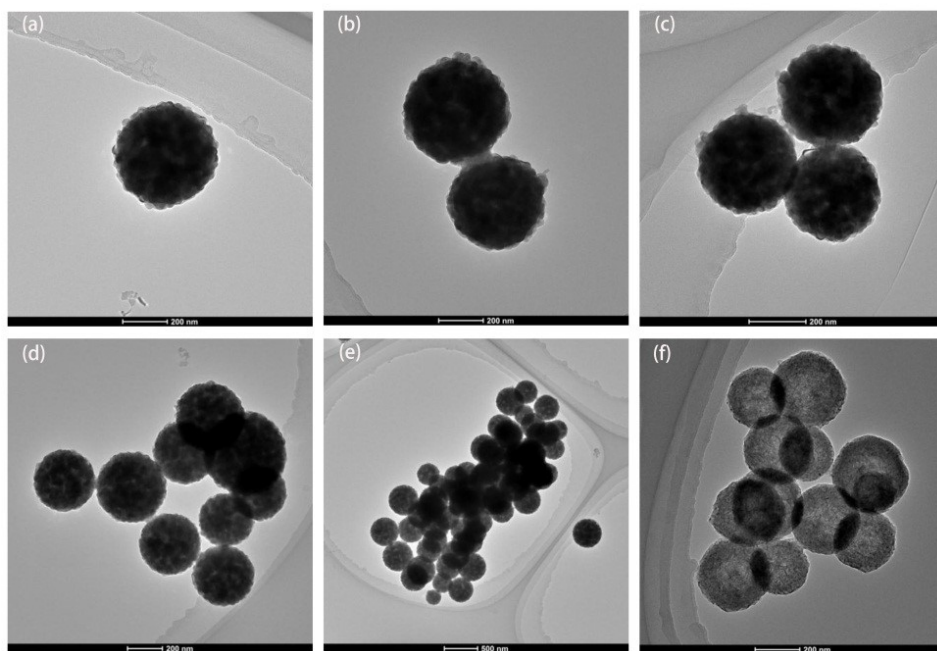


Fig. S9 TEM images of ZnO HMNSs (a), Zn_{1-x}Mg_xO HMNSs [$x = 0.012$ (b), $x = 0.030$ (c), $x = 0.052$ (d), $x = 0.089$ (e)], and MgO HMNSs (f).

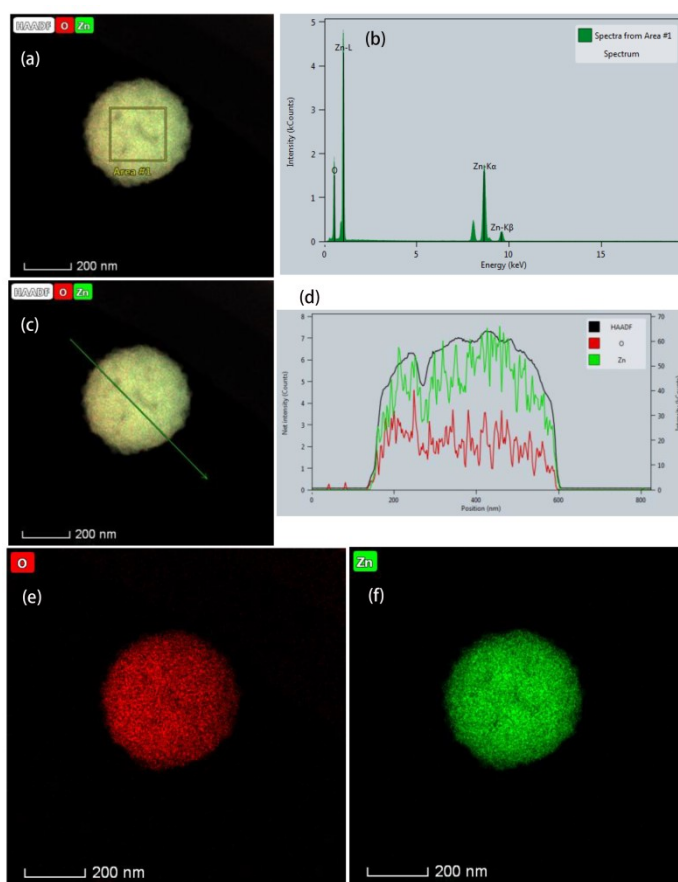


Fig. S10 HAADF image (a, c) with line scan profiles (d), EDX spectrum (b), and EDS maps (e:O, f:Zn) of ZnO HMNSs.

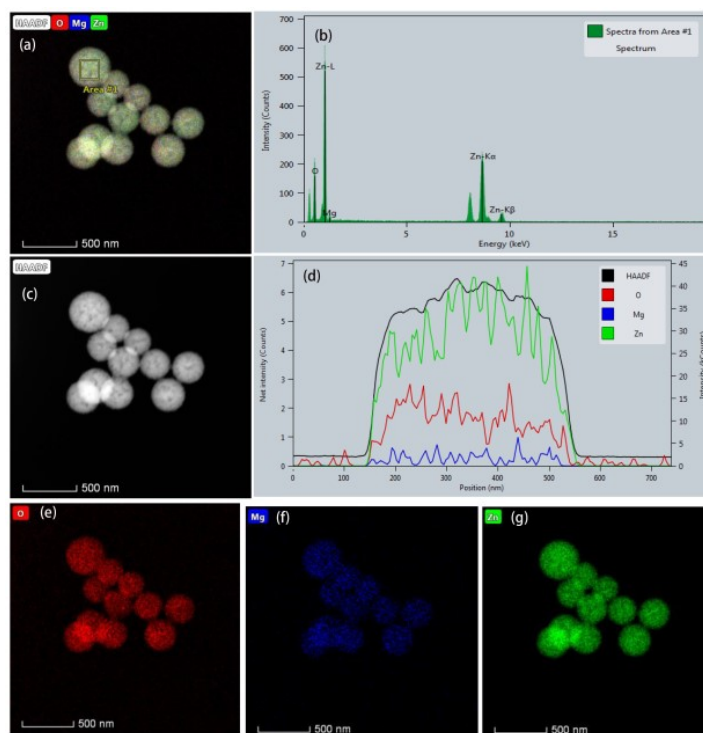


Fig. S11 HAADF image (a, c), EDX spectrum (b), and X-EDS maps (e: O, f: Mg, g: Zn) with line scan profiles (d) of Zn_{1-x}Mg_xO HMNSs (x = 0.052).

x Mg_xO HMNSs (x = 0.052).

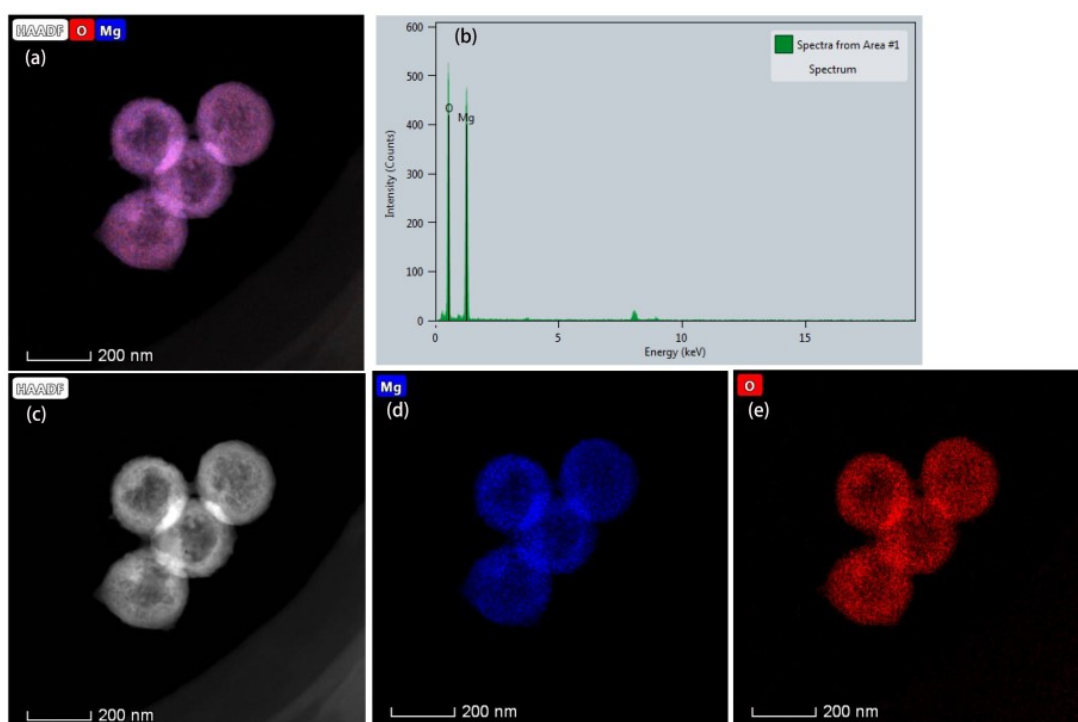


Fig. S12 HAADF image (a, c), EDX spectrum (b) and EDS maps (d, e) of MgO HMNSs.

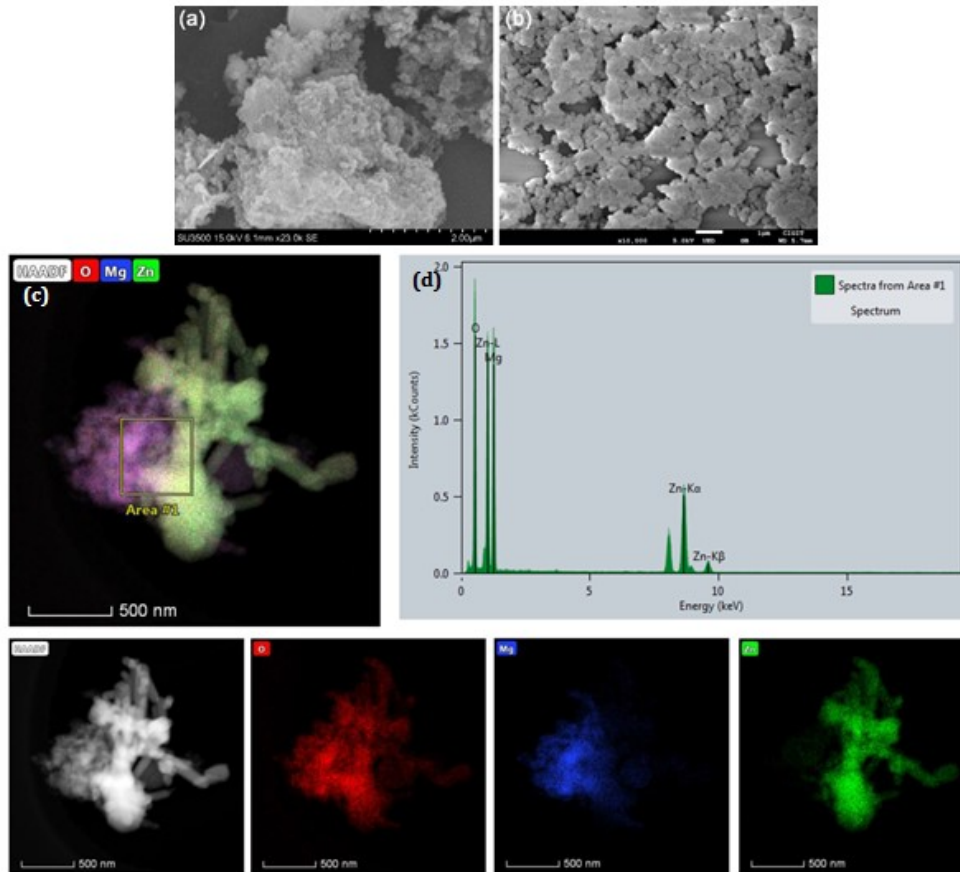


Fig. S13 SEM of ZnO-MgO(1:5) Cs (a) and ZnO-MgO(0.948:0.052) Cs (b), HAADF images and EDS maps (c), and EDX spectrum (d) of ZnO-MgO (1: 5) Cs.

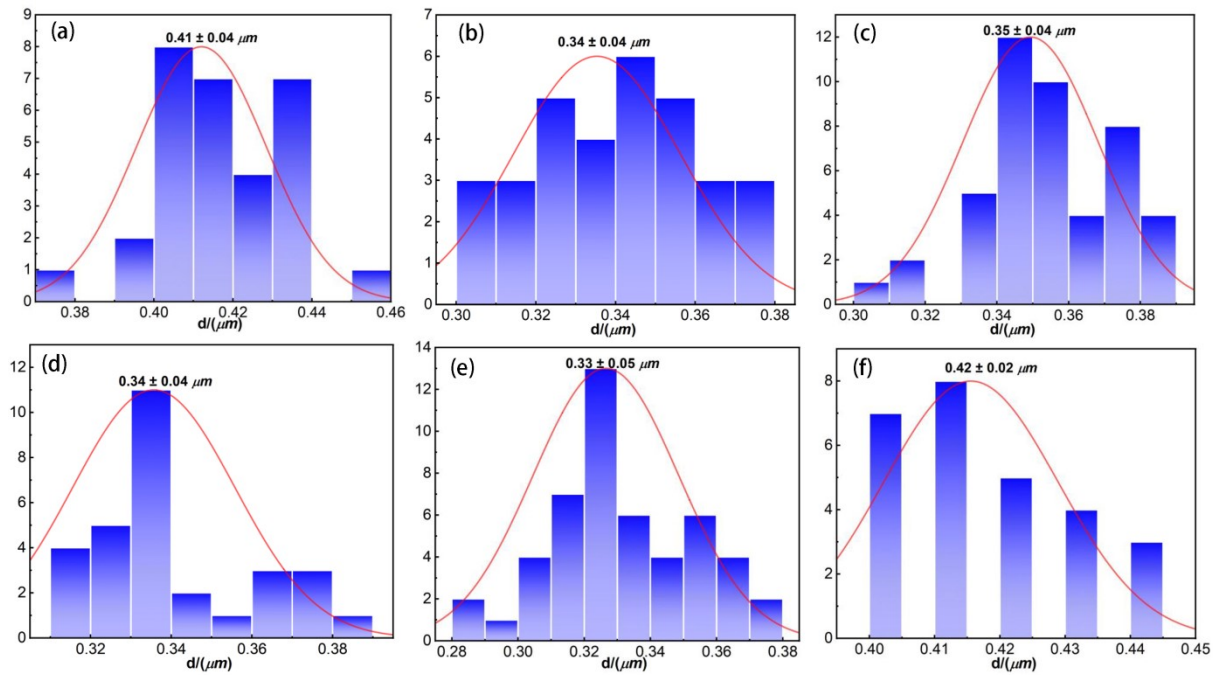


Fig. S14 Particle size distributions of Zn_{1-x}Mg_xO HMNSs (a: $x = 0.012$; b: $x = 0.030$; c: $x = 0.052$; d: $x = 0.089$), MgO NPs (e), and ZnO NPs (f).

(2) Structure

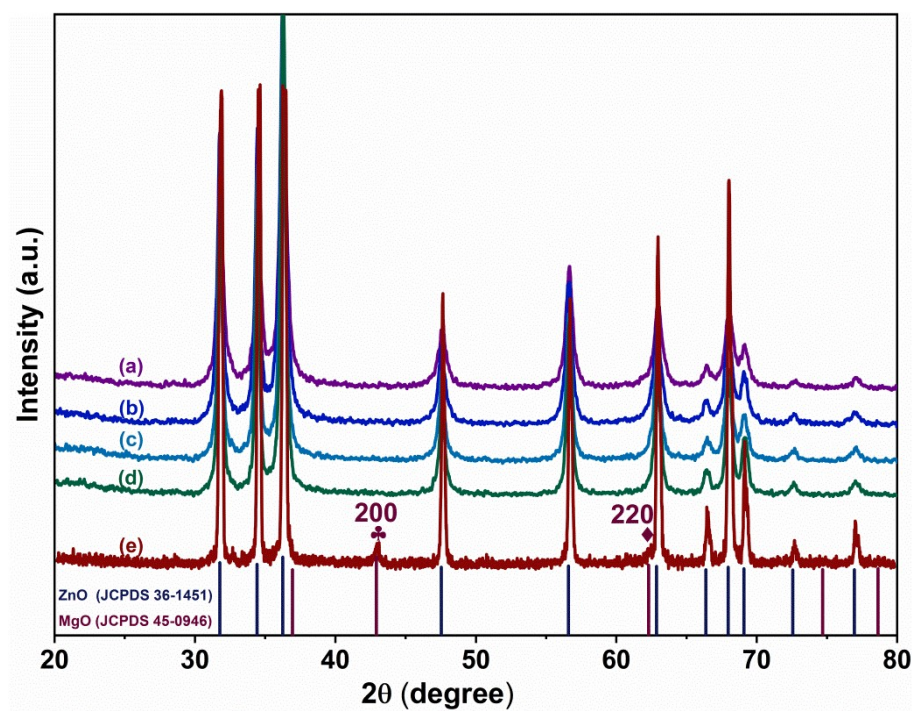


Fig. S15 Enlarged XRD patterns of $Zn_{1-x}Mg_xO$ HMNSs ($x = 0.012$) (a), $Zn_{1-x}Mg_xO$ HMNSs ($x = 0.030$) (b), $Zn_{1-x}Mg_xO$ HMNSs ($x = 0.052$) (c), $Zn_{1-x}Mg_xO$ HMNSs ($x = 0.089$) (d), and ZnO-MgO (0.948:0.052) Cs.

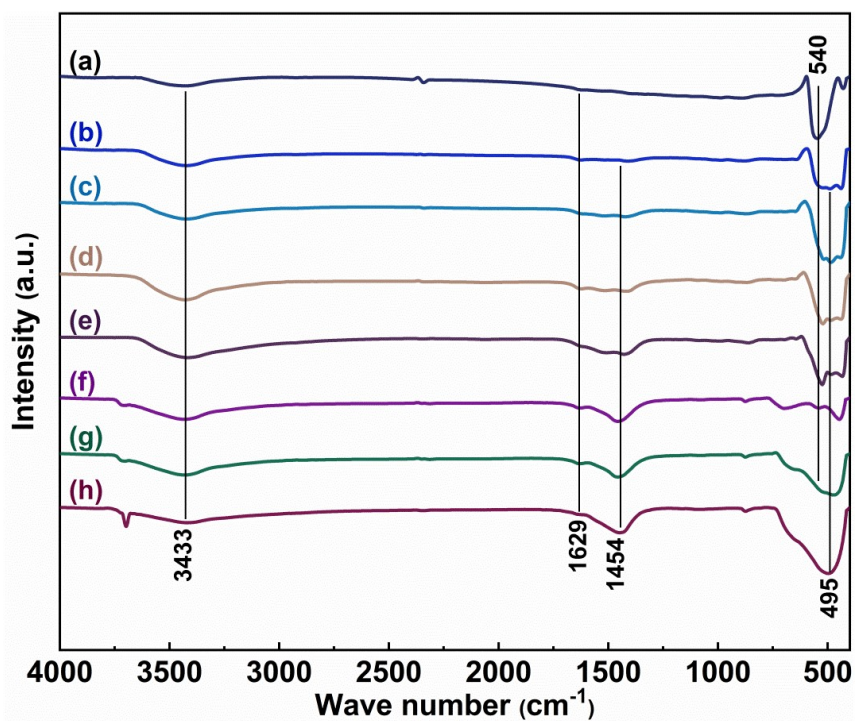


Fig. S16 FT-IR spectra of ZnO HMNSs (a), $Zn_{1-x}Mg_xO$ HMNSs ($x = 0.012$) (b), 0.030 (c), 0.052 (d), and 0.089 (e)), MgO HMNSs (f), ZnO-MgO(0.948:0.052) Cs (g), and ZnO-MgO(1:5) Cs (h).

Table S1 Structural parameters of ZnO HMNSs, Zn_{1-x}Mg_xO HMNSs ($x = 0.012, 0.030, 0.052, \text{ and } 0.089$), and MgO HMNSs calcined at 500°.

Parameter	ZnO HMNSs	Zn _{1-x} Mg _x O HMNSs			
		$x = 0.012$	0.030	0.052	0.089
2θ (002) (°)	34.42	34.42	34.44	34.45	34.46
D (nm)	44.6	39.0	28.9	23.2	19.0
FWHM (002)	0.21	0.29	0.32	0.34	0.43
c/a	1.606	1.602	1.600	1.598	1.595
ε (10^{-4})	20.9	29.5	32.9	39.7	45.9
δ ($10^{-4}/\text{nm}^2$)	5.0	6.6	12.0	18.6	27.7

(3) Textural Property

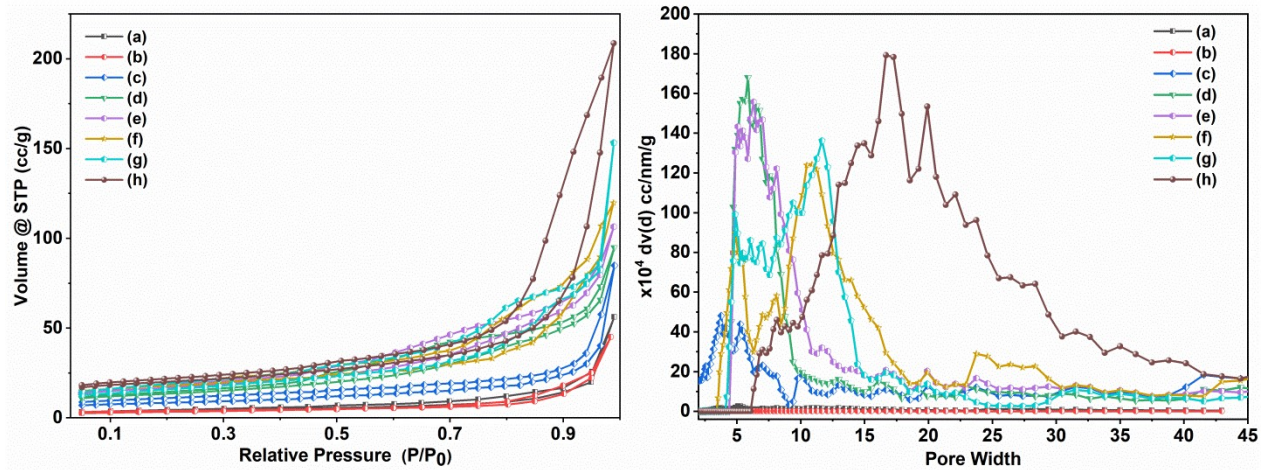


Fig. S17 N₂ adsorption-desorption isotherms (left) and pore size distributions (right) of ZnO-MgO (1:5) Cs (a), ZnO-MgO (0.948:0.052) Cs (b), ZnO HMNSs (c), Zn_{1-x}Mg_xO HMNSs ($x = 0.012$ (d), 0.030 (e), 0.052 (f), 0.089 (g)), and MgO HMNSs (h).

Table S2 Surface areas, average pore diameters and pore volumes of various catalysts.^a

Entry	Catalyst	Surface Area	Pore Volume	Average Pore Size	The Most Probable
		(m ² g ⁻¹) ^b	(cc g ⁻¹) ^c	(nm)	Pore Size (nm)
1	MgO HMNSs	45.9	0.31	27.0	17.3
2	Zn _{1-x} Mg _x O HMNSs (x = 0.012)	38.3	0.14	14.6	11.7
3	Zn _{1-x} Mg _x O HMNSs (x = 0.030)	45.4	0.16	14.1	10.9
4	Zn _{1-x} Mg _x O HMNSs (x = 0.052)	46.2	0.18	15.6	6.3
5	Zn _{1-x} Mg _x O HMNSs (x = 0.089)	39.7	0.18	18.1	5.9
6	ZnO HMNSs	22.7	0.13	22.9	3.8
7	ZnO-MgO (1:5) Cs	13.4	0.09	-	-
8	ZnO-MgO (0.948:0.052) Cs	10.8	0.07	-	-

^a N₂ adsorption-desorption is carried out at 77 K on a QUADRASORB SI020503 system, and the sample is degassed at 105 °C for 12 h before measurement. ^b Based on BET method. ^c Based on desorption data using DFT method ($P/P_0=0.990$).

(4) Amount and strength of basic/acidic sites

Table S3 Amounts and strengths of basic/acidic sites of Zn_{1-x}Mg_xO HMNSs (x = 0.012, 0.052 and 0.089) and ZnO-MgO (0.948:0.052) Cs.

Strength (°C)	Basic/acidic amount (mmol g ⁻¹)			
	Zn _{1-x} Mg _x O HMNSs			ZnO-MgO
	x = 0.012	0.052	0.089	(0.948:0.052) Cs
Medium (200-420)	0.58/0.64	1.39/0.66	2.27/2.27	0.42/0.63
Strong (420-650)	0.09/0.09	0.18/0.18	0.17/0.17	0.18/0.15
Super strong (650-820)	0.10/0.09	0.19/0.20	0.16/0.16	0.18/0.17

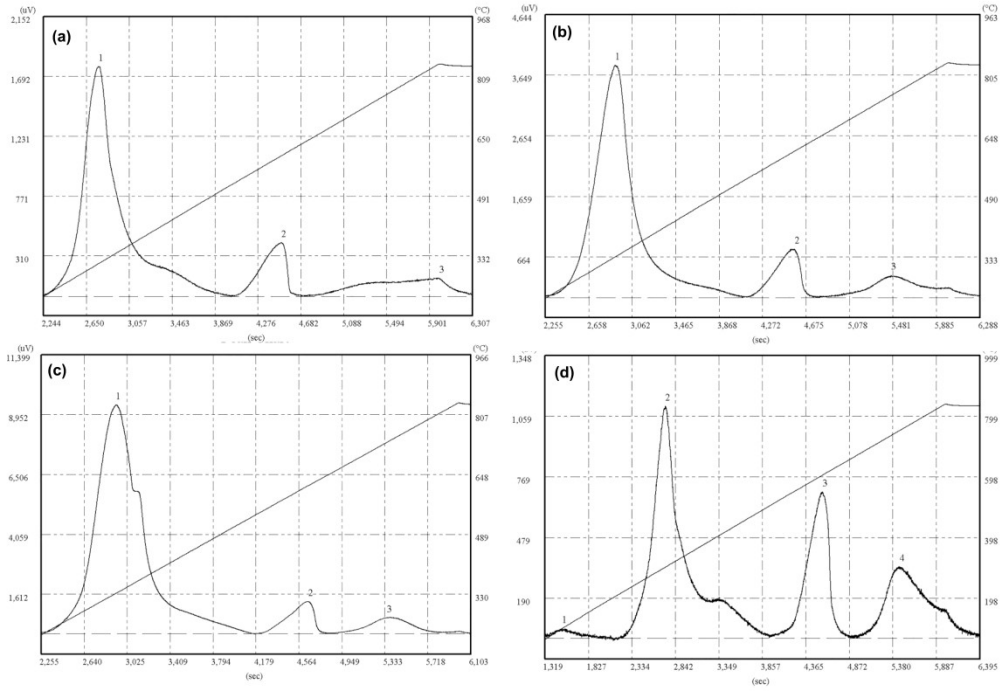


Fig. S18 CO₂-TPD curves of Zn_{1-x}Mg_xO HMNSs ($x = 0.012$ (a), 0.052 (b), 0.089 (c)) and ZnO-MgO (0.948:0.052) Cs.

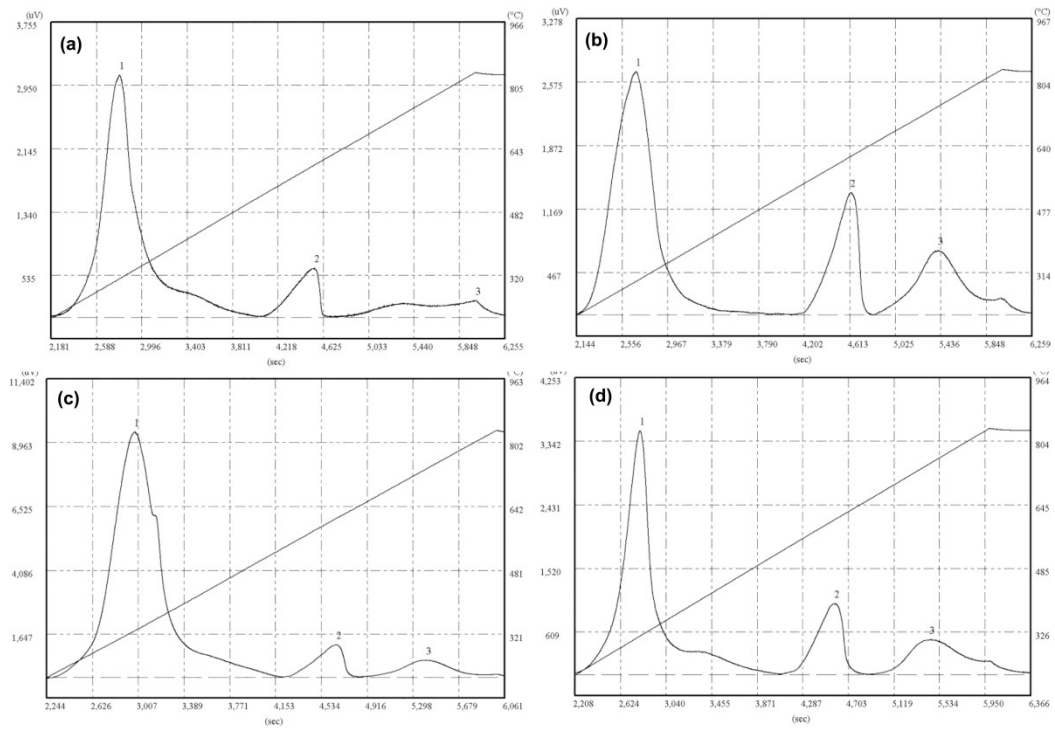


Fig. S19 NH₃-TPD curves of Zn_{1-x}Mg_xO HMNSs ($x = 0.012$ (a), 0.052 (b), 0.089 (c)) and ZnO-MgO (0.948:0.052) Cs.

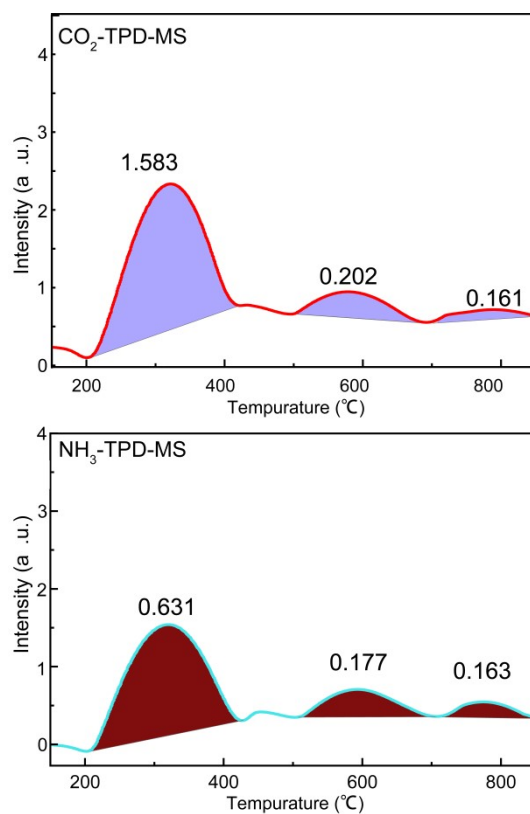


Fig. S20 TPD-MS curves of Zn_{1-x}Mg_xO HMNSs (x = 0.052).

(5) Type of acid sites (Lewis or Brønsted)

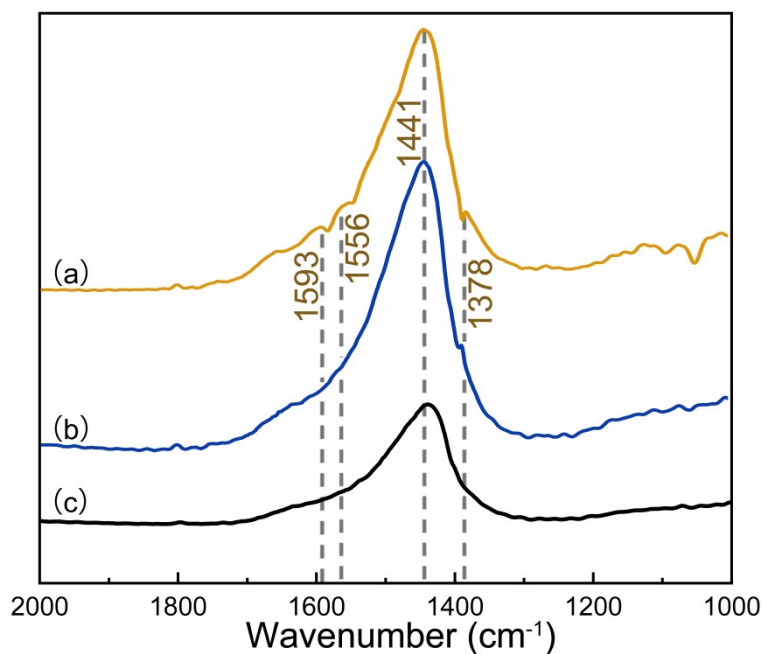


Fig. S21 IR spectra of pyridine-adsorbed Zn_{1-x}Mg_xO HMNSs (x = 0.052) vacuumized at 150 °C for 12 h (a), pyridine-adsorbed Zn_{1-x}Mg_xO HMNSs (x = 0.052) at r.t. (b), and Zn_{1-x}Mg_xO HMNSs (x = 0.052) (c).

4. Regio-selective O-methylation

(1) Optimization of reaction conditions

The effect of reaction conditions on catechol conversion and guaiacol selectivity in the O-methylation of catechol with DMC is investigated in detail and monitored by GC. First, a bivariate analysis with respect to temperature and mass ratio of catechol/catalyst is used to screen the optimal catechol conversion and guaiacol yield (Fig. S22a and Table S4). At mass ratios of catechol/catalyst = 16 and 12 at 160 °C, 180 °C and 200 °C, $Zn_{1-x}Mg_xO$ HMNSs ($x = 0.030$) promote the O-methylations of catechol in poor catechol conversion (< 22.1%) with low guaiacol yields (<14.7%). When the mass ratios decrease to 8 at 200 °C and 4 at 180 °C and 200 °C, a complete catechol conversion can be achieved. Among them, the best guaiacol yield (72.9%) is obtained at the mass ratio of catechol/catalyst = 4 at 180 °C. As the temperature increases to 200, veratrole is produced in 63.9% and 68.1% yields under the mass ratios at 6 and 4, respectively, indicating that a higher temperature is unfavorable for achieving high guaiacol selectivity. Moreover, the C-alkylated products are not obtained in all the O-methylations, and other unknown by-products in 0.1-16.0% yields are detected.

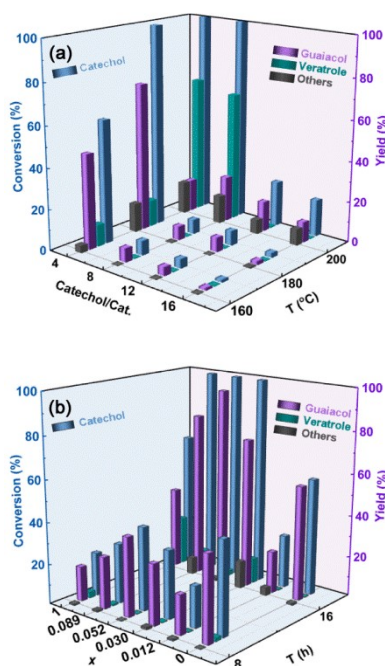


Fig. S22 Catechol conversion, guaiacol and by-product yields as functions of mass ratio of catechol/ $Zn_{1-x}Mg_xO$ HMNSs ($x = 0.030$) and temperature (a), and chemical composition (x) of $Zn_{1-x}Mg_xO$ HMNSs and reaction time (b).

At the mass ratio of catechol/catalyst = 4 at 180 °C, the guaiacol selectivity is optimized as functions of chemical composition (x) and reaction time. From Fig. S22b and Table S5, it is found that the chemical composition (x)

of $Zn_{1-x}Mg_xO$ HMNSs have a great impact on catechol conversion and guaiacol yield. When the x values are set to 1.0 and 0, the corresponding MgO HMNSs and ZnO HMNSs promote the O-methylations in 65.9% and 57.1% of catechol conversions within 16 h, respectively. It is worth noting that ZnO HMNSs shows a significantly higher guaiacol yield (97.9%) than MgO HMNSs (61.5%). After Mg ion is introduced into wurtzite ZnO to form a eutectic structure, all the as-prepared $Zn_{1-x}Mg_xO$ HMNSs with $x = 0.030, 0.052$ and 0.089 can achieve a complete catechol conversion within 16 h. Among them, $Zn_{1-x}Mg_xO$ HMNSs ($x = 0.052$) affords the highest guaiacol selectivity (94.5%) together with only 3.3% yield of veratrole within 16 h. However, all catalysts show the low catechol conversions (<45.1%) within 8 h. Moreover, the suitable molar ratio of DMC to catechol is further optimized. At the molar ratio of DMC/catechol = 4, the excellent guaiacol yield (95.5%) together with only 2.6% yield of veratrole and 1.9% yield of by-products is achieved (Table S6). Overall, the optimal conditions for highly regio-selective O-methylation of catechol with DMC to afford guaiacol in a complete catechol conversion with high guaiacol yield (95.5%) is summarized as follows: catechol (200.0 mg, 1.8 mmol), DMC (653.3 mg, 7.2 mmol), mass ratio of catechol/ $Zn_{1-x}Mg_xO$ HMNSs ($x = 0.052$) = 4, 180 °C, 16 h.

Table S4 Influence of mass ratio of catechol/catalyst and reaction temperature on catechol conversion, selectivity and yield of product and by-product in the methylation of catechol.^a

Entry	Catechol /catalyst ^b	Temp. (°C)	Catechol conv. ^c (%)	Product selectivity/yield (%/%) ^c			
				Veratrole	Guaiacol	C-alkylated	Others
1	16	160	1.1	9.4 /0.1	82.8 /0.9	-	7.8/0.1
2	16	180	2.2	2.0 /<0.1	74.5/1.6	-	23.5 /0.5
3	16	200	18.0	0.9 /0.2	55.2/9.9	-	43.9/7.9
4	12	160	4.3	3.3/0.1	92.0/4.0	-	4.7/0.2
5	12	180	7.0	0.5/<0.1	98.7/6.9	-	0.8/<0.1
6	12	200	22.1	2.1/0.5	66.5/14.7	-	31.4/6.9
7	8	160	6.9	2.3/0.2	95.6/6.6	-	2.1/0.1
8	8	180	7.0	-	95.4/6.7	-	4.6/0.3
9	8	200	100	63.9/63.9	22.3/22.3	-	13.8/13.8
10	4	160	60.3	17.5/10.6	76.9/46.4	-	5.6/3.4
11	4	180	100	13.0/13.0	72.9/72.9	-	14.1/14.1
12	4	200	100	68.1/68.1	15.9/15.9	-	16.0/16.0

^a Reaction conditions: Catechol (200.0 mg, 1.8 mmol), DMC (490 mg, 5.4 mmol), $Zn_{1-x}Mg_xO$ HMNSs ($x = 0.030$), 16 h. ^b Mass ratio of catechol/Catalyst. ^c Determined by GC.

Table S5 Effect of chemical composition of $Zn_{1-x}Mg_xO$ HMNSs and reaction time on catechol conversion, product selectivity and product yield in the methylation of catechol.^a

Entry	x	Time (h)	Catechol conv. ^b (%)	Product selectivity/Yield (%/%) ^b			
				Veratrole	Guaiachol	C-alkylated	Others
1	1.0 ^c	8	21.7	17.9/3.9	81.3/17.6	-	0.7/0.2
2	1.0 ^c	16	65.9	37.2/24.5	61.5/40.5	-	1.3/0.9
3	0.089	8	29.4	6.1/1.8	87.8/25.8	-	6.1/1.8
4	0.089	16	100	10.5/10.5	80.4/80.4	-	9.1/9.1
5	0.052	8	40.7	2.9/1.2	95.1/38.7	-	2.0/0.8
6	0.052	16	100	3.3/3.3	94.5/94.5	-	2.1/2.1
7	0.030	8	33.3	4.2 /1.4	89.4/29.8	-	6.4/2.1
8	0.030	16	100	3.0/3.0	92.9/92.9	-	4.1/4.1
9	0.012	8	20.6	4.0/0.8	95.2/19.6	-	0.8/0.2
10	0.012	16	68.2	3.1/2.1	94.1/64.2	-	2.8/1.9
11	0 ^d	8	45.1	6.1/2.7	92.0/41.5	-	2.0/0.9
12	0 ^d	16	57.1	2.1/1.2	97.9/55.9	-	-

^a Reaction conditions: Catechol (200.0 mg, 1.8 mmol), DMC (490 mg, 5.4 mmol), mass ratio of catechol/catalyst = 4, 180 °C. ^b Determined by GC. ^c MgO HMNPs. ^d ZnO HMNPs.

Table S6 Effect of molar ratios of DMC to catechol on catechol conversions, product selectivities and product yields in the methylation reaction of catechol with DMC.^a

Entry	Molar DMC/catechol	Catechol conv. ^b (%)	Product selectivity (%) ^b			
			Veratrole	Guaiachol	C-alkylated	Others
1	1.0	100	39.2	38.0	-	22.8
2	2.0	100	46.2	31.5	-	22.3
3	3.0	100	3.3	94.5	-	2.1
4	4.0	100	2.6	95.5	-	1.9
5	5.0	100	10.7	81.4	-	7.9

^a Reaction conditions: Catechol (200.0 mg, 1.8 mmol), mass ratio of catechol/ $Zn_{1-x}Mg_xO$ HMNSs ($x = 0.052$) = 4:1, 180 °C, 16 h. ^b Determined by GC

(2) Catalytic performances of various acid-base catalysts

Table S7 Catechol conversions, product yields and product selectivities catalyzed by various catalysts in the methylation reactions of catechol.^a

Entry	Catalyst	Catechol conv. ^b (%)	Product selectivity/Yield (%/%) ^b			
			Veratrole	Guaiachol	C-alkylated	Others
1	ZnO HMNSs	57.1	1.9/1.1	95.7/54.6	-	2.3/1.3
2	ZnO-MgO (1:5) Cs	83.9	46.2/38.8	51.4/43.1	-	2.5/2.0
3	ZnO-MgO (0.948:0.052) Cs	77.4	3.5/2.7	93.3/72.2	-	3.2/2.5
4	Zn _{1-x} Mg _x O HMNSs (x = 0.052)	100	2.6/2.6	95.5/95.5	-	1.9/1.9
5	MgO HMNSs	65.9	37.2/24.5	61.5/40.5	-	1.3/0.9
6 ^c	ZnO HMNSs + MgO HMNSs	56.7	2.8/1.6	94.0/53.3	-	3.2/1.8

^a Reaction conditions: Catechol (200.0 mg, 1.8 mmol), DMC (653.3 mg, 7.2 mmol), mass ratio of catechol/catalyst = 4:1, 180 °C, 16 h. ^b Determined by GC. ^c Molar ratio of ZnO HMNSs/MgO HMNSs = 0.948:0.052.

(3) Reaction kinetics

Table S8 Concentrations of catechol, guaiachol and veratrole in the whole methylation process of catechol catalyzed by various catalysts.^a

Time (h)	Catechol concentration (mmol L ⁻¹) ^b			Guaiachol/veratrole concentration (mmol L ⁻¹) ^b		
	Zn _{1-x} Mg _x O HMNSs (x = 0.052)	ZnO-MgO (0.948:0.052) Cs	ZnO-MgO (1:5) Cs	Zn _{1-x} Mg _x O HMNSs (x = 0.052)	ZnO-MgO (0.948:0.052) Cs	ZnO-MgO (1:5) Cs
0	18	18	18	0/0	0/0	0/0
2	15.6	16.9	17.3	2.1/0.1	0.9/0.0	0.7/0.0
4	12.9	16.0	16.3	4.9/0.1	1.9/0.1	1.2/0.4
6	12.0	15.1	15.3	5.8/0.2	3.5/0.1	1.4/0.5
8	10.7	13.9	14.0	7.0/0.2	4.8/0.1	2.2/1.6
10	7.8	12.7	12.3	9.6/0.3	6.4/0.1	3.0/2.7
12	3.8	10.8	9.8	13.5/0.5	8.6/0.2	4.1/3.1
14	2.0	6.9	6.3	15.2/0.6	10.8/0.2	6.2/5.2
16	0	4.1	2.9	17.0/0.6	12.7/0.2	7.8/7.0

^a Reaction conditions: Catechol (200.0 mg, 1.8 mmol), DMC (653.3 mg, 7.2 mmol), mass ratio of catechol/catalyst = 4, 180 °C. ^b Determined by GC.

(4) Substrate scope

Table S9 Substrate conversions and product selectivities/yields in the alkylation of diphenols.^a

Entry	Substrate conv. (%) ^b	Product selectivity/Yield (%/%) ^b			
		Mono-ether		Di-ether	Others
1 ^a	 94.5	 94.3/89.1	 5.7/5.4	-	
2 ^a	 100	 95.3/95.3	 2.7/2.7	2.0/2.0	
3 ^a	 100	 89.0/89.0	 4.0/4.0	7.2/7.2	
4 ^a	 100	 92.8/92.8	 0.6/0.6	6.6/6.6	
5 ^a	 82.6	 67.8/56.0	 19.3/15.9	12.9/10.7	
6 ^a	 94.6	 65.5/61.9	 33.6/31.8	0.9/0.9	
7 ^c	 49.8	 60.9/30.3	 0.6/0.3	38.5/19.2	
8 ^c	 48.3	 64.9/31.3	 4.4/2.1	30.7/14.8	
9 ^c	 54.1	 59.7/32.3	 3.2/1.7	37.1/20.1	

^a Reaction conditions: molar ratio of substrate/DMC = 1/4, Zn_{1-x}Mg_xO HMNSs (x = 0.052), 180 °C, 16 h. ^b Determined by GC. ^c Reaction conditions: molar ratio of substrate/DEC = 1/4, Zn_{1-x}Mg_xO HMNSs (x = 0.052), 180 °C, 16 h

(5) Reusability of catalyst

Table S10 Catechol conversions, selectivities/yields of guaiacol and veratrole in the Zn_{1-x}Mg_xO HMNSs (x = 0.052)-promoted O-methylation of catechol with DMC in repeated test.^a

Reuse times	Catechol conv. ^b (%)	Product selectivity ^b /Yield (%/%) ^c			
		Veratrole	Guaiacol	C-alkylated	Others
1	100	2.6/2.6	95.5/95.5	-	1.9/-
	(88.9) ^d	(2.2/2.0) ^d	(96.2/85.5) ^d		(1.6/-) ^d
2	99.5	7.5/7.4	92.1/91.8	-	0.4/-
	(88.6) ^d	(6.8/6.0) ^d	(92.8/82.2) ^d		(0.4/-) ^d
3	99.4	8.0/7.8	91.5/91.3	-	0.4/-
	(88.4) ^d	(7.6/6.7) ^d	(92.1/81.4) ^d		(0.3/-) ^d
4	97.9	10.6/10.1	87.9/86.5	-	1.5/-
	(87.9) ^d	(10.3/9.1) ^d	(88.5/77.8) ^d		(1.2/-) ^d

5	96.9 (87.1) ^d	16.8/16.1 (16.5/14.4) ^d	81.2/78.6 (81.8/71.2) ^d	2.0/- (1.7) ^d
6	95.9 (86.4) ^d	26.5/24.5 (25.9/22.4) ^d	71.0/68.7 (71.8/62.0) ^d	- (2.3/-) ^d

^a Reaction conditions: Zn_{1-x}Mg_xO HMNSs (x = 0.052), catechol (1.00 g, 9.0 mmol), DMC (2.61 g, 28.8 mmol), molar ratio of catechol/DMC = 1/4, 180 °C, 16 h. ^b Selectivity of product is calculated according to the percent of total peak areas of products, respectively. ^c Determined by GC: guaiacol and veratrole yields are determined quantitatively by internal standard method and area normalization, respectively. ^d Data collected at the reaction time of 14 h.

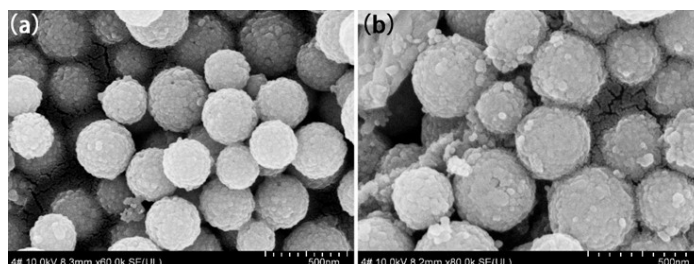


Fig. S23 SEM images of fresh (a) and 6th-reused Zn_{1-x}Mg_xO HMNSs (x= 0.052) (b).

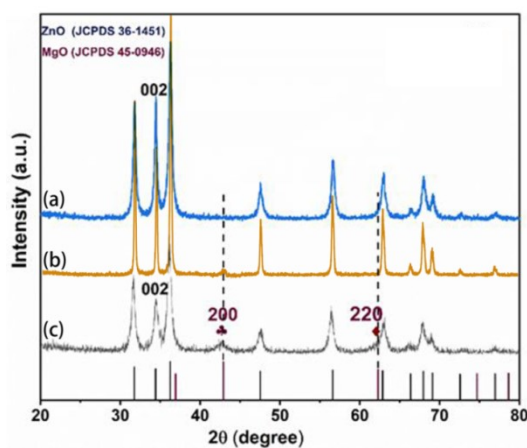


Fig. S24 XRD patterns of fresh (a), 4th-reused (b) and 6th-reused (c) Zn_{1-x}Mg_xO HMNSs (x= 0.052).

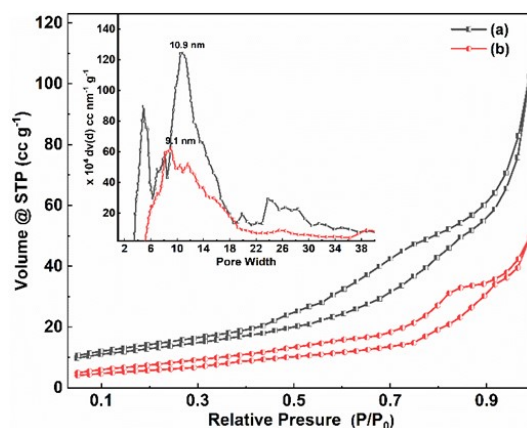


Fig. S25 N₂ adsorption-desorption isotherms and pore size distributions of the fresh (a) and 6th-reused Zn_{1-x}Mg_xO HMNSs (x= 0.052) (b).

5. Activation model of ZnO HMNSs and MgO HMNSs

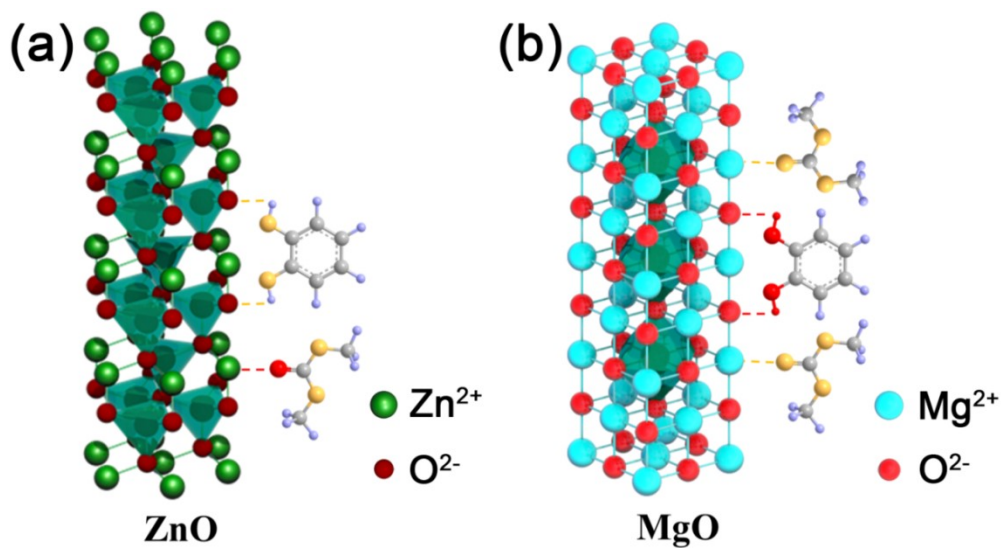


Fig. S26 Proposed activation models of ZnO HMNSs (a) and MgO HMNSs (b) for catechol and DMC.

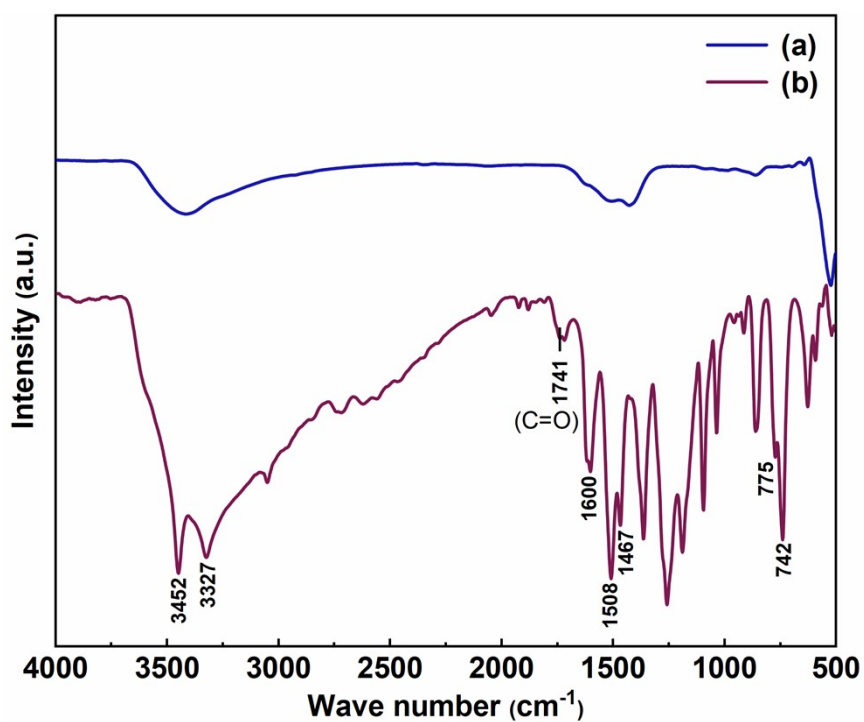
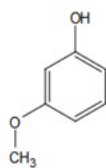
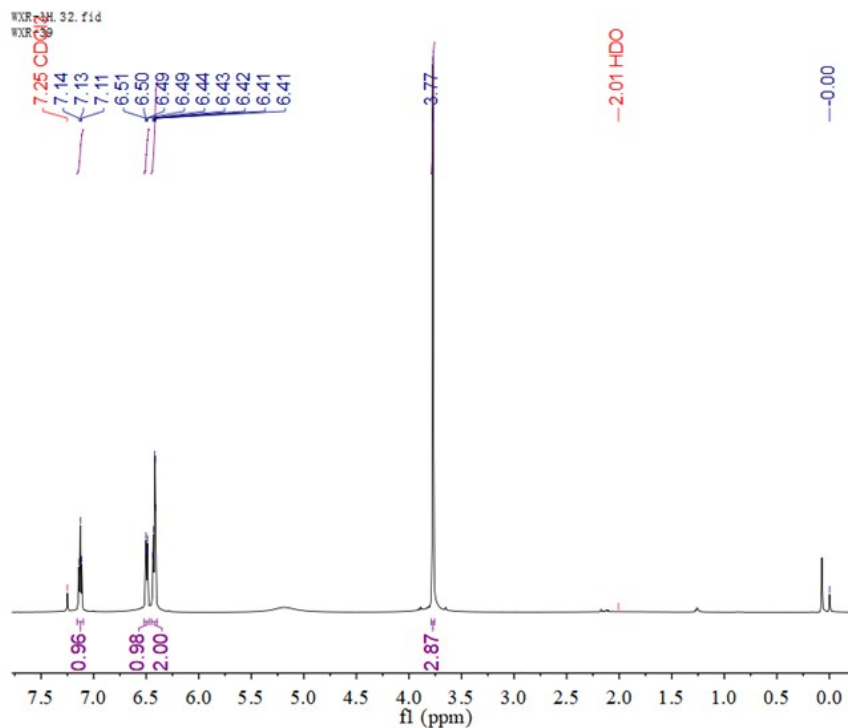


Fig. S27 FT-IR spectra of Zn_{1-x}Mg_xO HMNSs ($x = 0.052$) (a) and DMC/catechol-adsorbed Zn_{1-x}Mg_xO HMNSs ($x = 0.052$).

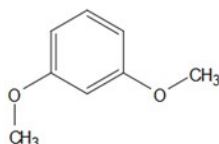
6. ¹H NMR spectra of products



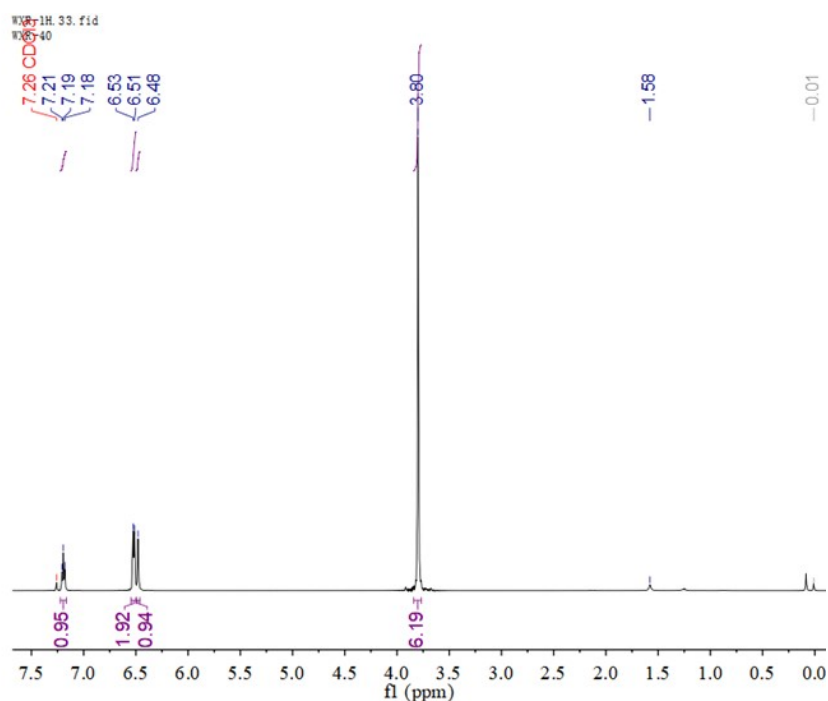
Parameter	值
1 Origin	Bruker BioSpin GmbH
2 Instrument	spect
3 Solvent	CDCl3
4 Temperature	465.9
5 Pulse Sequence	zg30
6 Experiment	1D
7 Probe	5 mm PABBO BB/ 19F-1H/ D Z-GRD Z114607/ 0142
8 Number of Scans	16
9 Presaturation Frequency	
10 Acquisition Time	2.7263
11 Acquisition Date	2020-12-17T10:17:00
12 Modification Date	2020-12-17T10:17:00
13 Spectrometer Frequency	600.13
14 Nucleus	1H



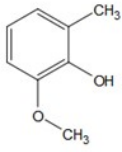
¹H NMR (600 MHz, Chloroform-d) δ 7.13 (t, *J* = 8.0 Hz, 1H), 6.50 (dt, *J* = 8.2, 2.3 Hz, 1H), 6.45 – 6.40 (m, 2H), 5.18 (s, 1H), 3.77 (s, 3H), 3.74 (s, 1H).



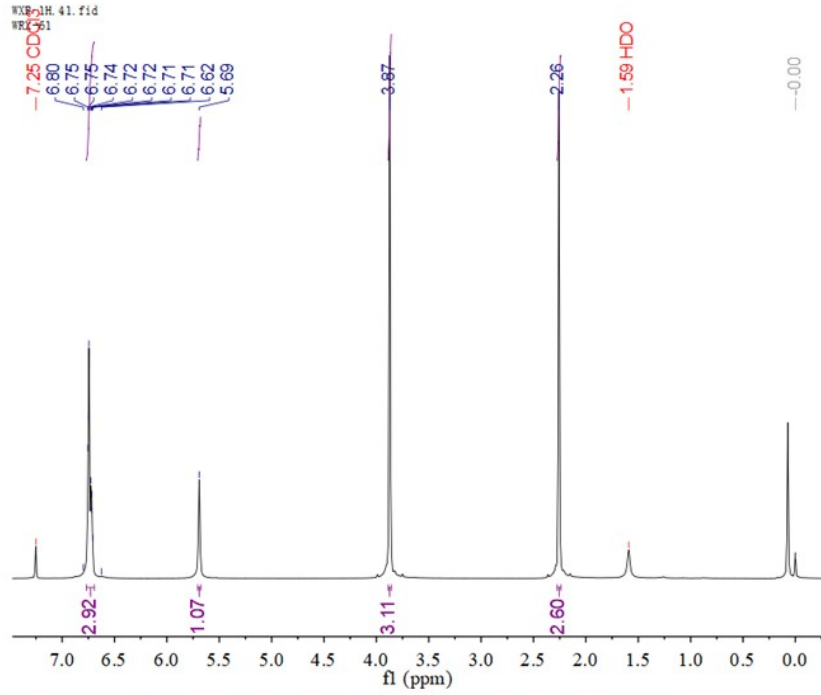
Parameter	Value
1 Origin	Bruker BioSpin GmbH
2 Instrument	spect
3 Solvent	CDCl3
4 Temperature	477.0
5 Pulse Sequence	zg30
6 Experiment	1D
7 Probe	5 mm PABBO BB/ 19F-1H/ D Z-GRD Z114607/ 0142
8 Number of Scans	16
9 Presaturation Frequency	
10 Acquisition Time	2.7263
11 Acquisition Date	2020-12-17T10:21:00
12 Modification Date	2020-12-17T10:21:00
13 Spectrometer Frequency	600.13
14 Nucleus	1H



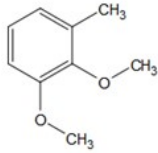
¹H NMR (600 MHz, Chloroform-d) δ 7.19 (t, *J* = 8.4 Hz, 1H), 6.52 (d, *J* = 8.3, 2.4 Hz, 2H), 6.48 (t, *J* = 2.3 Hz, 1H), 3.80 (s, 6H).



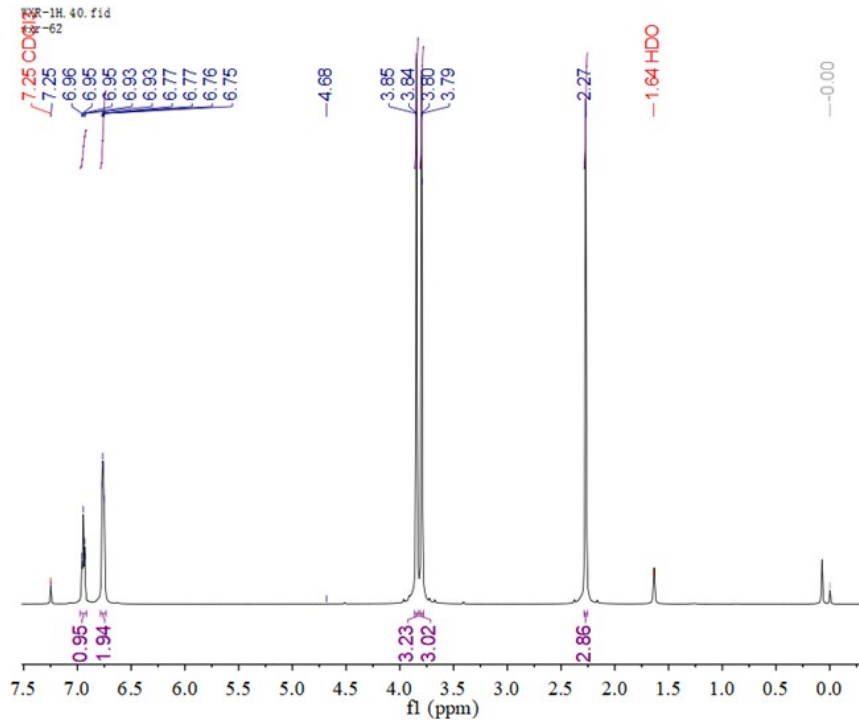
Parameter	值
1 Origin	Bruker BioSpin GmbH
2 Instrument	spect
3 Solvent	CDCl3
4 Temperature	296.9
5 Pulse Sequence	zg30
6 Experiment	1D
7 Probe	5 mm PABBO BB/ 19F-1H/ D Z-GRD Z114607/ 0142
8 Number of Scans	16
9 Presaturation Frequency	
10 Acquisition Time	2.7263
11 Acquisition Date	2021-03-18T10:01:00
12 Modification Date	2021-03-18T10:02:02
13 Spectrometer Frequency	600.13
14 Nucleus	1H



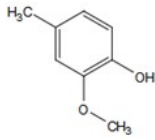
$^1\text{H NMR}$ (600 MHz, Chloroform-*d*) δ 6.77 – 6.69 (m, 3H), 5.69 (s, 1H), 3.87 (s, 3H), 2.26 (s, 3H).



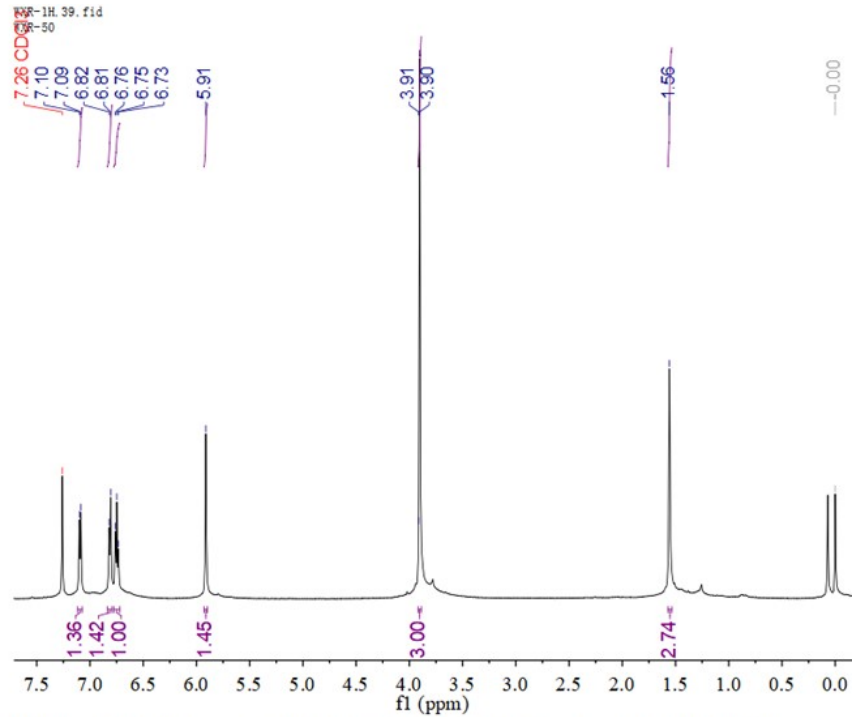
Parameter	值
1 Origin	Bruker BioSpin GmbH
2 Instrument	spect
3 Solvent	CDCl3
4 Temperature	297.2
5 Pulse Sequence	zg30
6 Experiment	1D
7 Probe	5 mm PABBO BB/ 19F-1H/ D Z-GRD Z114607/ 0142
8 Number of Scans	16
9 Presaturation Frequency	
10 Acquisition Time	2.7263
11 Acquisition Date	2021-03-18T09:21:00
12 Modification Date	2021-03-18T09:21:34
13 Spectrometer Frequency	600.13
14 Nucleus	1H



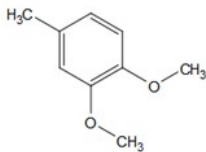
$^1\text{H NMR}$ (600 MHz, Chloroform-*d*) δ 6.95 (t, $J = 7.8$ Hz, 1H), 6.79 – 6.73 (m, 2H), 3.84 (d, $J = 2.0$ Hz, 3H), 3.80 (d, $J = 2.0$ Hz, 3H), 2.27 (s, 3H).



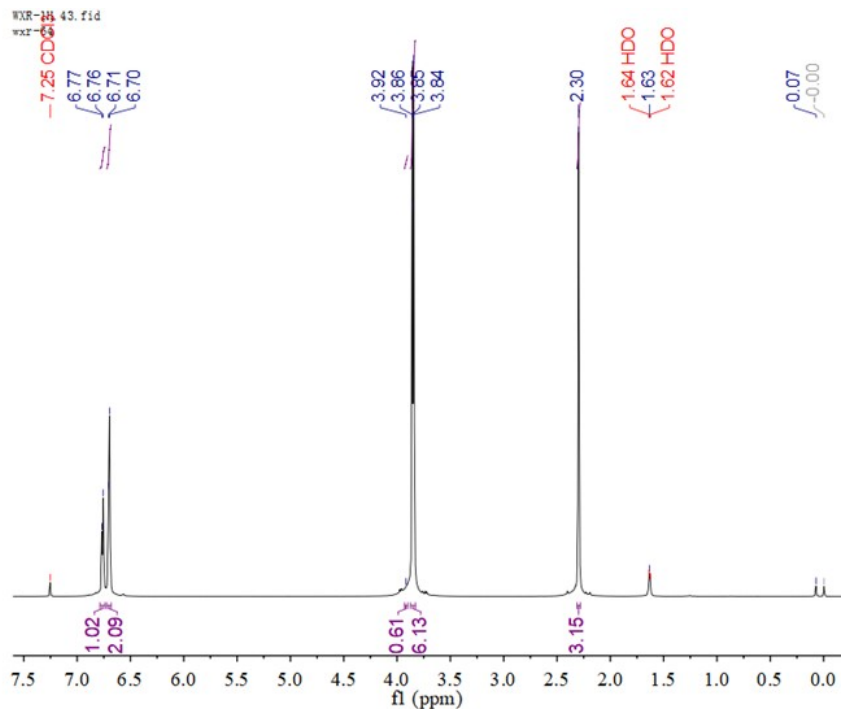
Parameter	值
1 Origin	Bruker BioSpin GmbH
2 Instrument	spect
3 Solvent	CDCl3
4 Temperature	301.0
5 Pulse Sequence	zg30
6 Experiment	1D
7 Probe	5 mm PABBO BB/ 19F-1H/ D Z-GRD Z114607/0142
8 Number of Scans	16
9 Presaturation Frequency	
10 Acquisition Time	2.7263
11 Acquisition Date	2021-03-11T13:30:00
12 Modification Date	2021-03-11T13:30:46
13 Spectrometer Frequency	600.13
14 Nucleus	1H



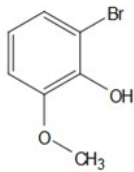
$^1\text{H NMR}$ (600 MHz, Chloroform-*d*) δ 7.12 – 7.07 (m, 1H), 6.83 – 6.79 (m, 1H), 6.78 – 6.72 (m, 1H), 5.91 (d, 1H), 3.90 (s, 3H), 1.56 (s, 3H).



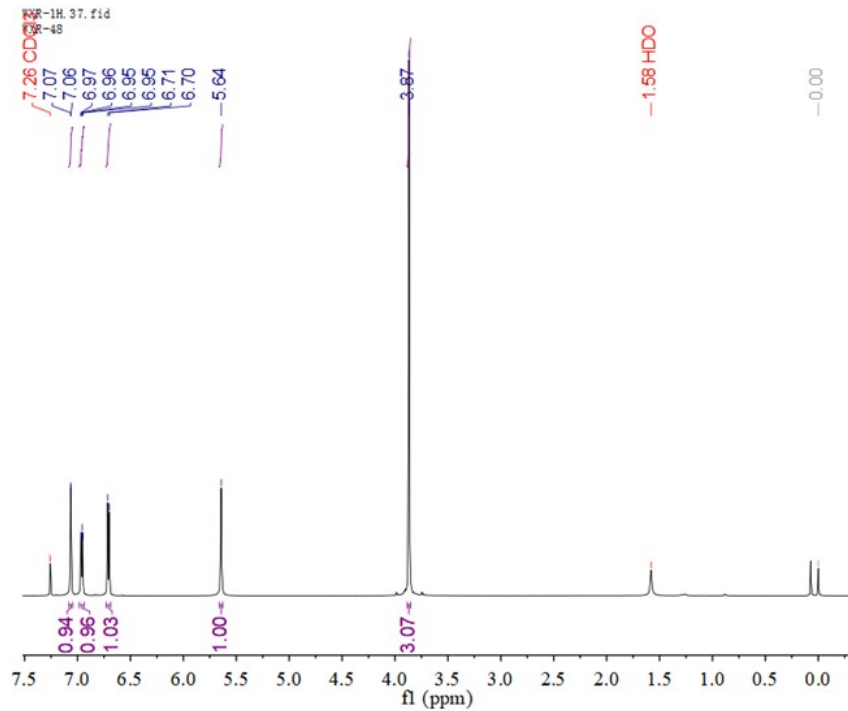
Parameter	值
1 Origin	Bruker BioSpin GmbH
2 Instrument	spect
3 Solvent	CDCl3
4 Temperature	297.1
5 Pulse Sequence	zg30
6 Experiment	1D
7 Probe	5 mm PABBO BB/ 19F-1H/ D Z-GRD Z114607/0142
8 Number of Scans	16
9 Presaturation Frequency	
10 Acquisition Time	2.7263
11 Acquisition Date	2021-03-18T09:29:00
12 Modification Date	2021-03-18T09:29:26
13 Spectrometer Frequency	600.13
14 Nucleus	1H



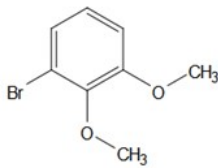
$^1\text{H NMR}$ (600 MHz, Chloroform-*d*) δ 6.78 – 6.74 (m, 1H), 6.72 – 6.68 (m, 2H), 3.92 (s, 1H), 3.85 (d, $J = 8.5$ Hz, 6H), 2.30 (s, 3H).



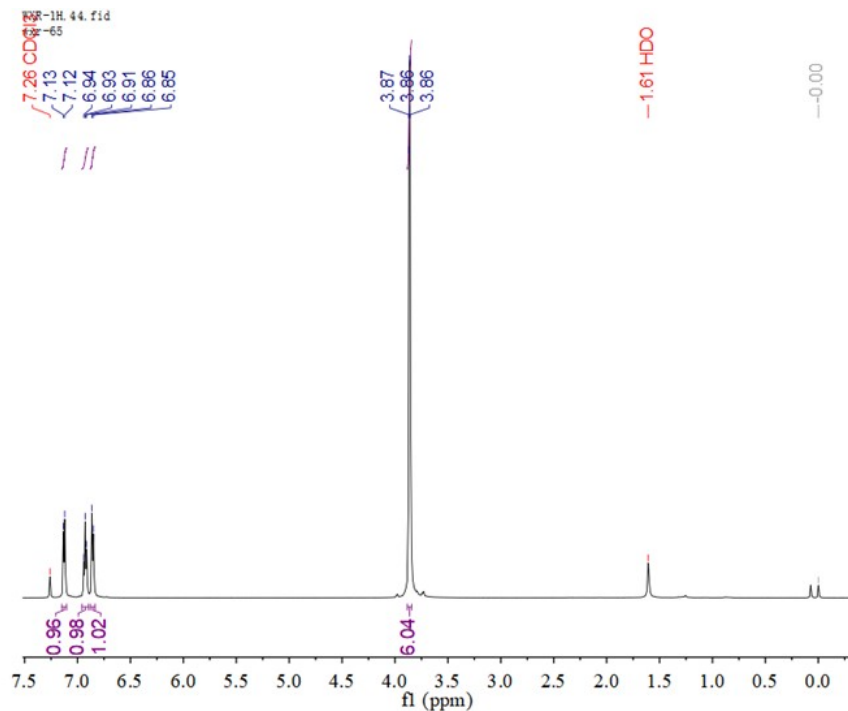
Parameter	值
1 Origin	Bruker BioSpin GmbH
2 Instrument	spect
3 Solvent	CDCl3
4 Temperature	301.4
5 Pulse Sequence	zg30
6 Experiment	1D
7 Probe	5 mm PABBO BB/ 19F-1H/ D Z-GRD Z114607/0142
8 Number of Scans	16
9 Presaturation Frequency	
10 Acquisition Time	2.7263
11 Acquisition Date	2021-03-11T16:22:00
12 Modification Date	2021-03-11T16:22:40
13 Spectrometer Frequency	600.13
14 Nucleus	1H



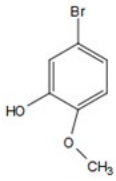
$^1\text{H NMR}$ (600 MHz, Chloroform-*d*) δ 7.06 (d, $J = 2.4$ Hz, 1H), 6.96 (dd, $J = 8.7, 2.4$ Hz, 1H), 6.71 (d, $J = 8.6$ Hz, 1H), 5.64 (s, 1H), 3.87 (s, 3H).



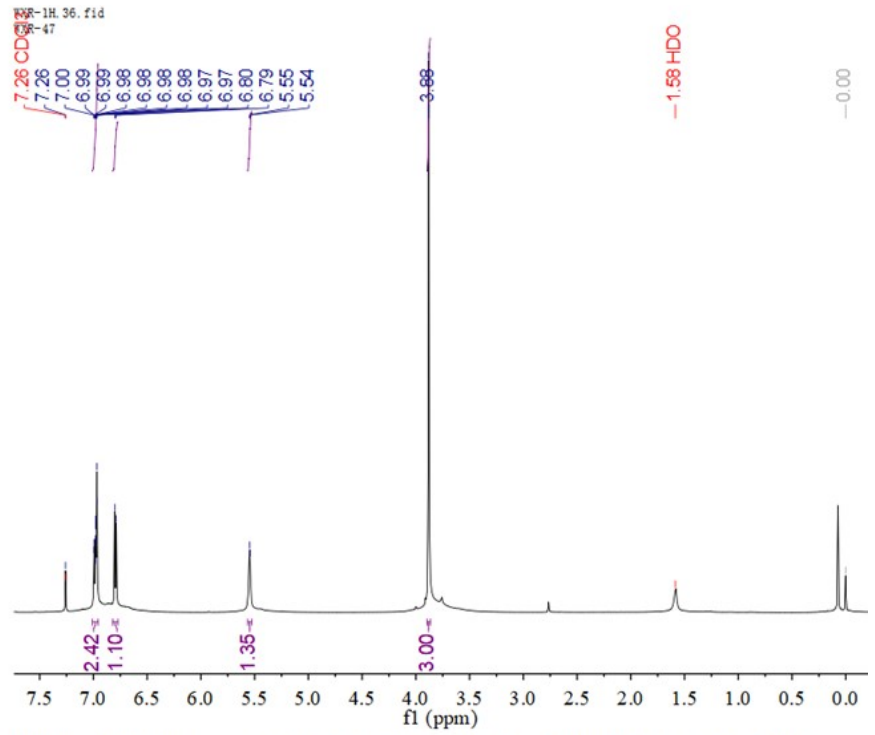
Parameter	值
1 Origin	Bruker BioSpin GmbH
2 Instrument	spect
3 Solvent	CDCl3
4 Temperature	297.1
5 Pulse Sequence	zg30
6 Experiment	1D
7 Probe	5 mm PABBO BB/ 19F-1H/ D Z-GRD Z114607/0142
8 Number of Scans	16
9 Presaturation Frequency	
10 Acquisition Time	2.7263
11 Acquisition Date	2021-03-18T09:33:00
12 Modification Date	2021-03-18T09:33:52
13 Spectrometer Frequency	600.13
14 Nucleus	1H



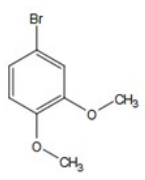
$^1\text{H NMR}$ (600 MHz, Chloroform-*d*) δ 7.13 (d, $J = 8.1$ Hz, 1H), 6.93 (t, $J = 8.3$ Hz, 1H), 6.86 (d, $J = 8.2$ Hz, 1H), 3.88 – 3.84 (m, 6H).



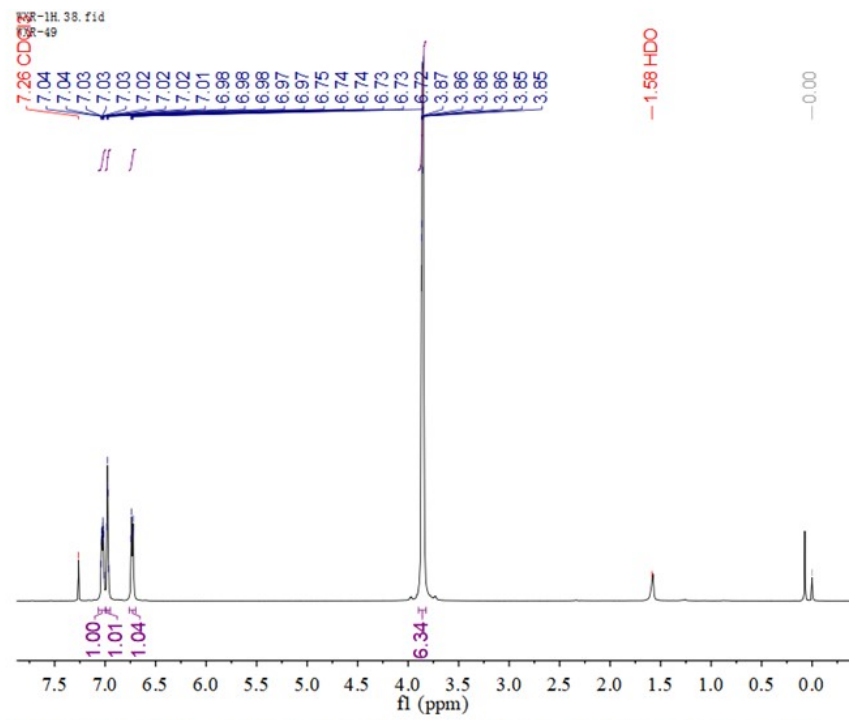
Parameter	值
1 Origin	Bruker BioSpin GmbH
2 Instrument	spect
3 Solvent	CDCl3
4 Temperature	301.6
5 Pulse Sequence	zg30
6 Experiment	1D
7 Probe	5 mm PABBO BB/19F-1H/ D Z-GRD Z114607/0142
8 Number of Scans	16
9 Presaturation Frequency	
10 Acquisition Time	2.7263
11 Acquisition Date	2021-03-11T13:17:00
12 Modification Date	2021-03-11T13:17:46
13 Spectrometer Frequency	600.13
14 Nucleus	1H



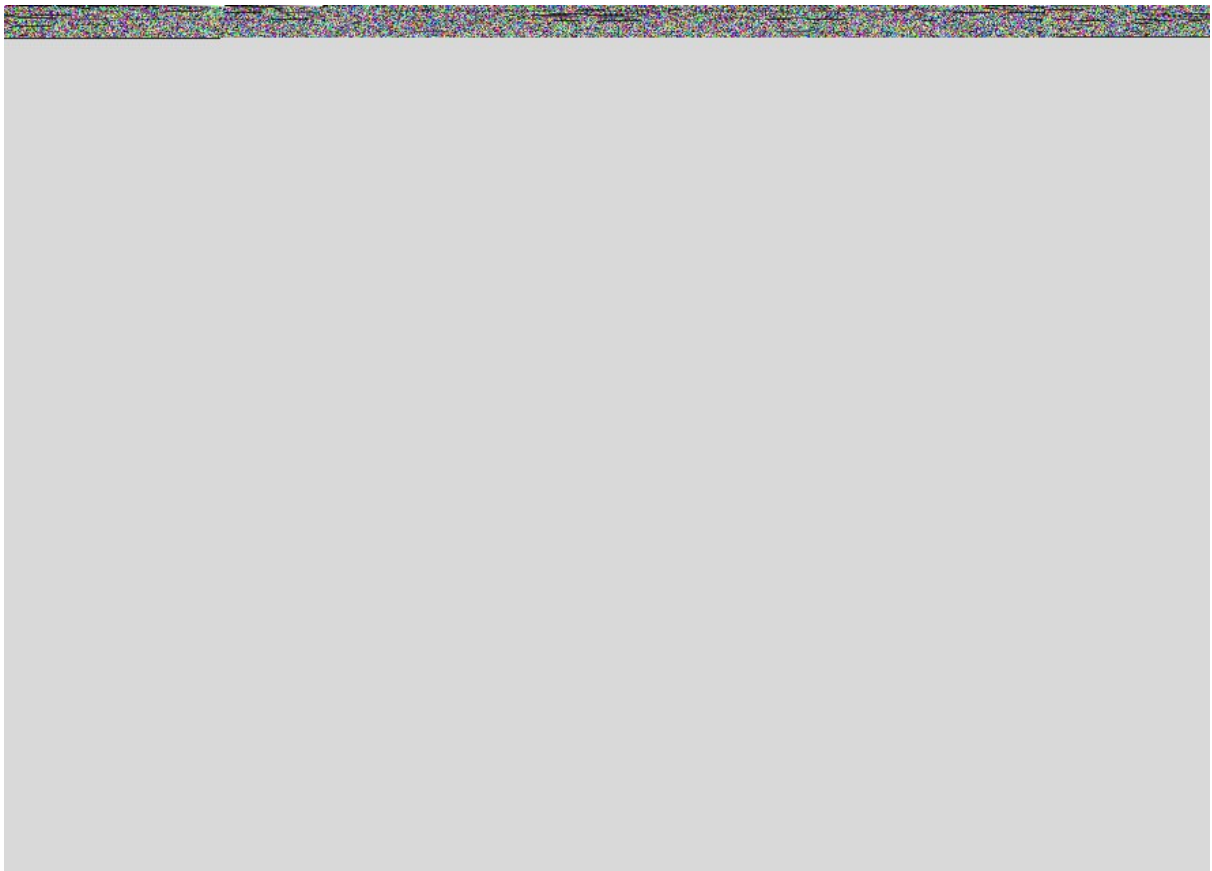
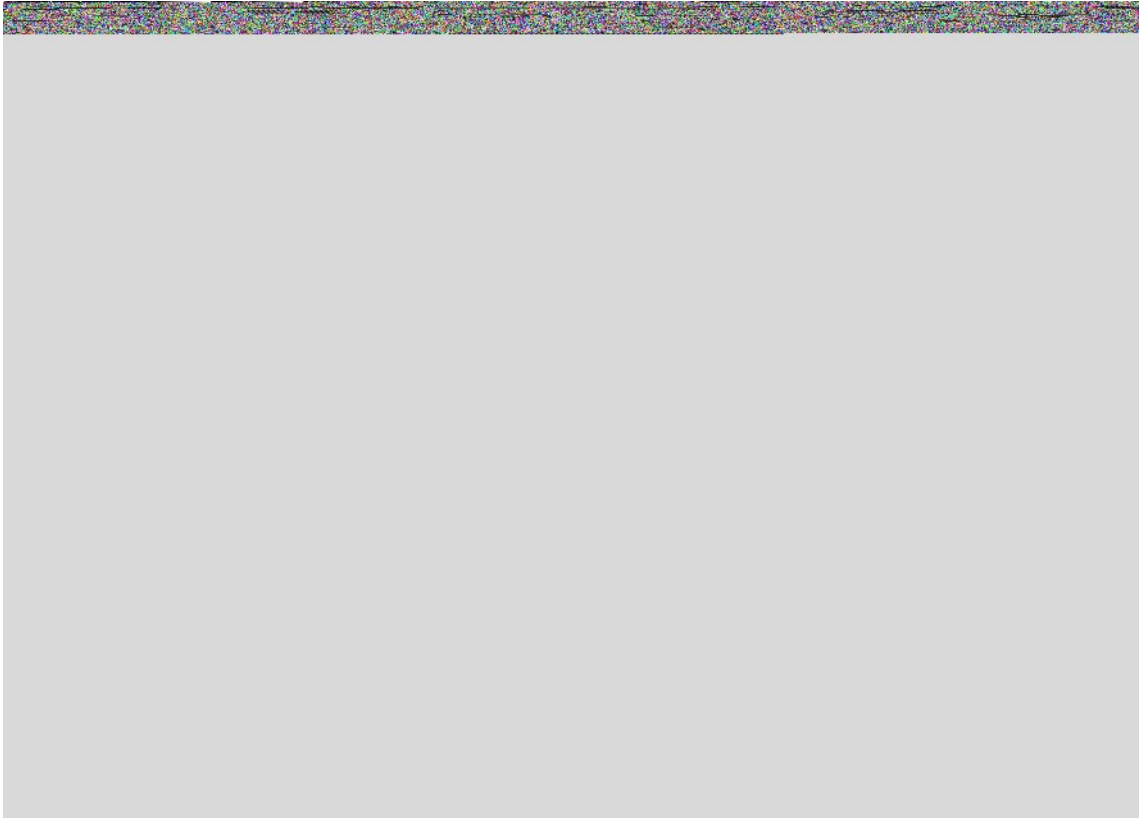
¹H NMR (600 MHz, Chloroform-*d*) δ 7.01 – 6.96 (m, 2H), 6.80 (d, *J* = 8.4, 1.2 Hz, 1H), 5.55 (d, *J* = 3.9 Hz, 1H), 3.88 (s, 3H).

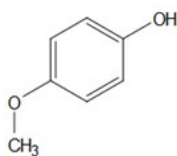


Parameter	值
1 Origin	Bruker BioSpin GmbH
2 Instrument	spect
3 Solvent	CDCl3
4 Temperature	301.1
5 Pulse Sequence	zg30
6 Experiment	1D
7 Probe	5 mm PABBO BB/19F-1H/ D Z-GRD Z114607/0142
8 Number of Scans	16
9 Presaturation Frequency	
10 Acquisition Time	2.7263
11 Acquisition Date	2021-03-11T13:26:00
12 Modification Date	2021-03-11T13:26:12
13 Spectrometer Frequency	600.13
14 Nucleus	1H

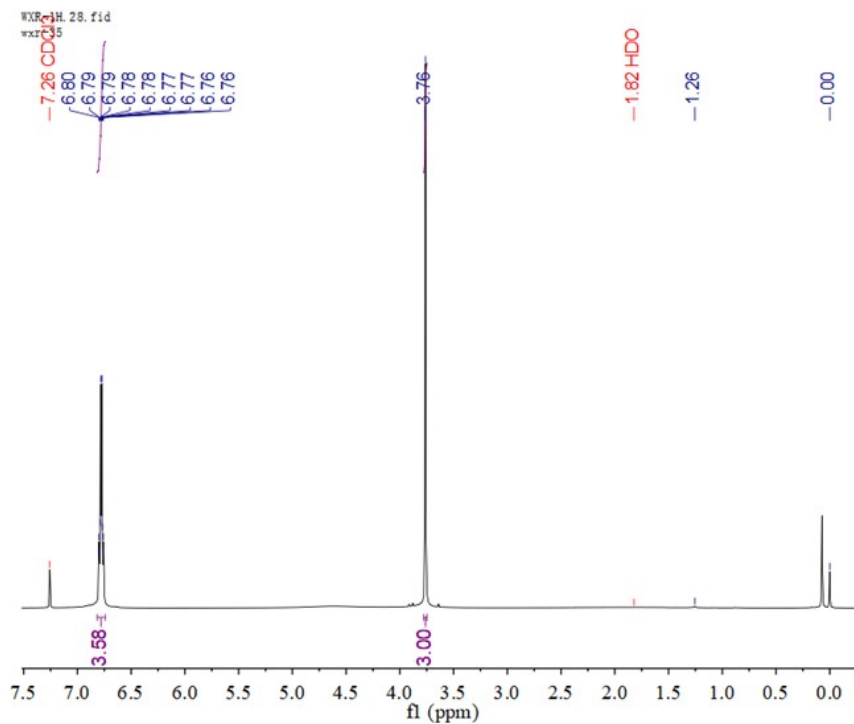


¹H NMR (600 MHz, Chloroform-*d*) δ 7.07 – 6.99 (m, 1H), 7.00 – 6.95 (m, 1H), 6.76 – 6.70 (m, 1H), 3.90 – 3.82 (m, 6H).

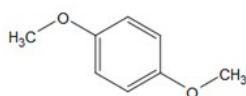




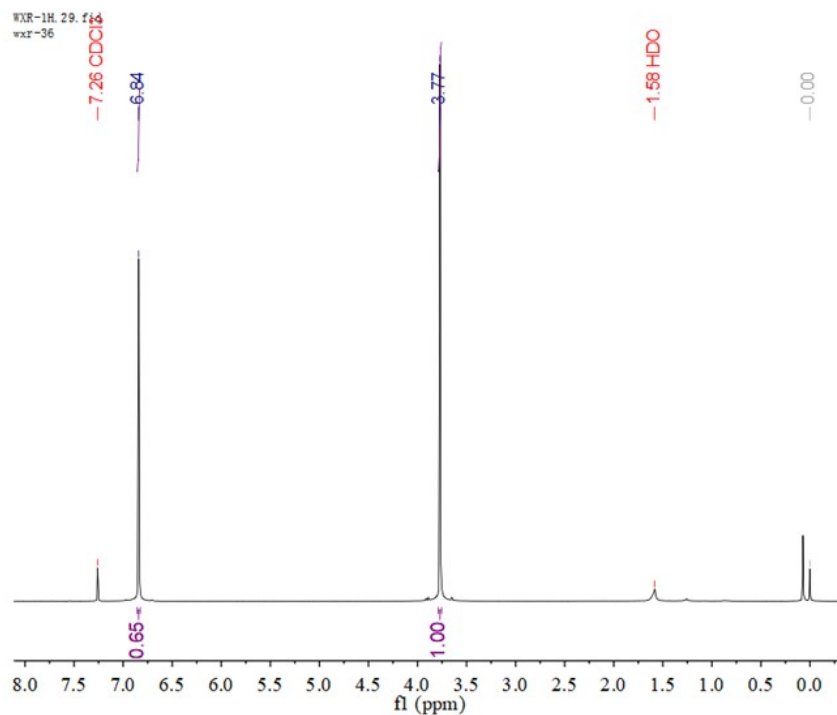
Parameter	值
1 Origin	Bruker BioSpin GmbH
2 Instrument	spect
3 Solvent	CDCl3
4 Temperature	497.7
5 Pulse Sequence	zg30
6 Experiment	1D
7 Probe	5 mm PABBO BB/ 19F-1H/ D Z-GRD Z114607/0142
8 Number of Scans	16
9 Presaturation Frequency	
10 Acquisition Time	2.7263
11 Acquisition Date	2020-12-14T07:48:00
12 Modification Date	2020-12-14T07:48:00
13 Spectrometer Frequency	600.13
14 Nucleus	1H



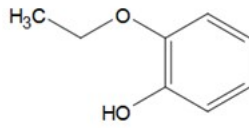
$^1\text{H NMR}$ (600 MHz, Chloroform-*d*) δ 6.82 – 6.74 (m, 4H), 3.76 (s, 3H).



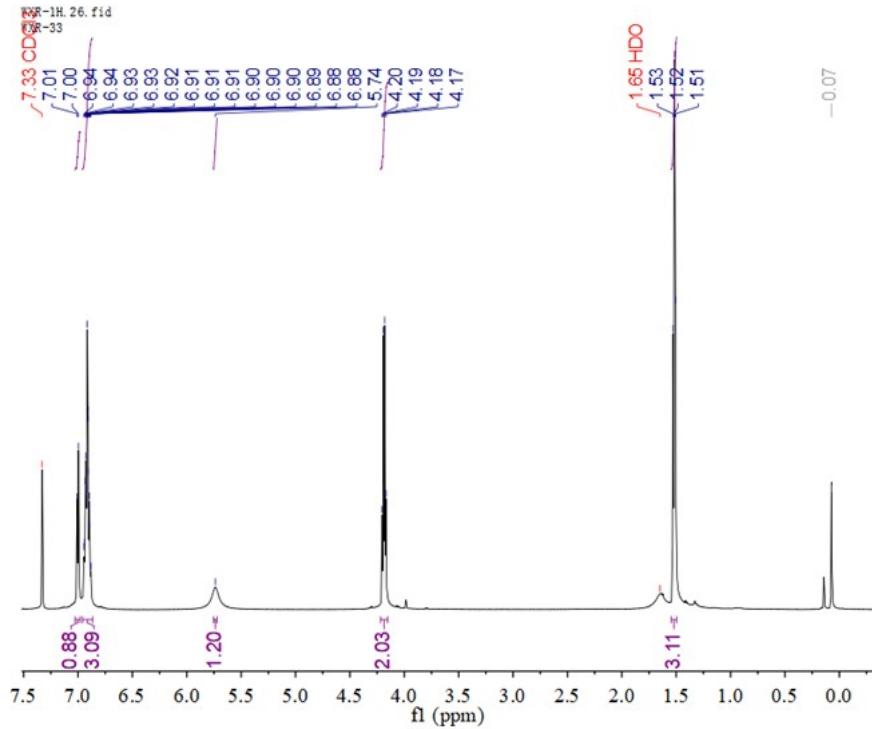
Parameter	Value
1 Origin	Bruker BioSpin GmbH
2 Instrument	spect
3 Solvent	CDCl3
4 Temperature	501.8
5 Pulse Sequence	zg30
6 Experiment	1D
7 Probe	5 mm PABBO BB/ 19F-1H/ D Z-GRD Z114607/0142
8 Number of Scans	16
9 Presaturation Frequency	
10 Acquisition Time	2.7263
11 Acquisition Date	2020-12-14T07:52:00
12 Modification Date	2020-12-14T07:52:00
13 Spectrometer Frequency	600.13
14 Nucleus	1H



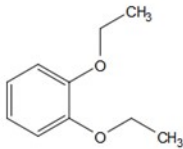
$^1\text{H NMR}$ (600 MHz, Chloroform-*d*) δ 6.84 (s, 1H), 3.77 (s, 1H).



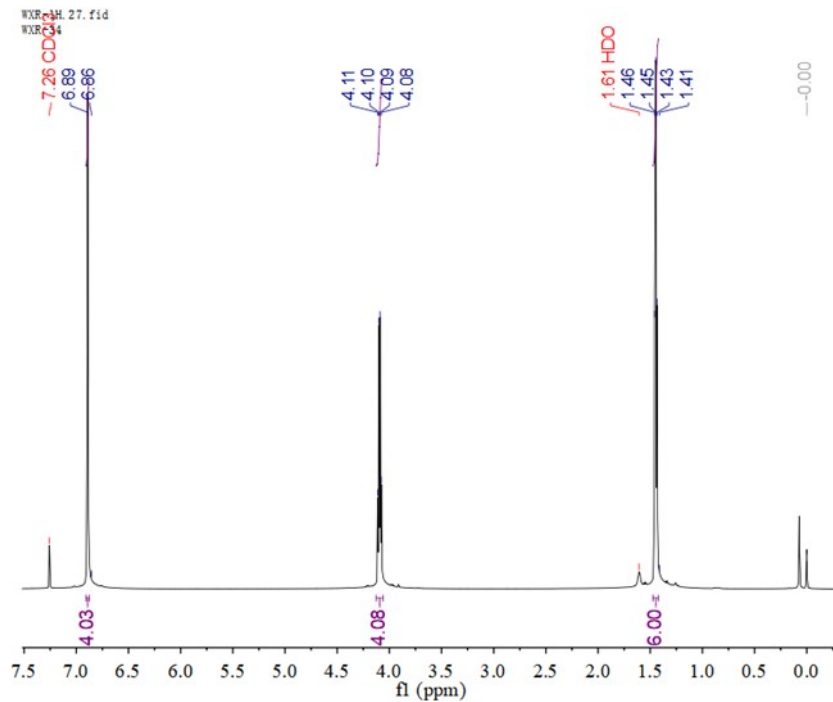
Parameter	值
1 Origin	Bruker BioSpin GmbH
2 Instrument	spect
3 Solvent	CDCl3
4 Temperature	498.5
5 Pulse Sequence	zg30
6 Experiment	1D
7 Probe	5 mm PABBO BB/ 19F-1H/ D Z-GRD Z114607/0142
8 Number of Scans	16
9 Presaturation Frequency	
10 Acquisition Time	2.7263
11 Acquisition Date	2020-12-03T02:31:00
12 Modification Date	2020-12-03T02:31:00
13 Spectrometer Frequency	600.13
14 Nucleus	1H



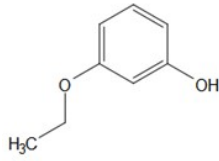
$^1\text{H NMR}$ (600 MHz, Chloroform- d) δ 7.00 (d, $J = 7.3$ Hz, 1H), 6.96 – 6.87 (m, 3H), 5.74 (s, 1H), 4.19 (q, $J = 7.0$ Hz, 2H), 1.52 (t, $J = 7.0$ Hz, 3H).



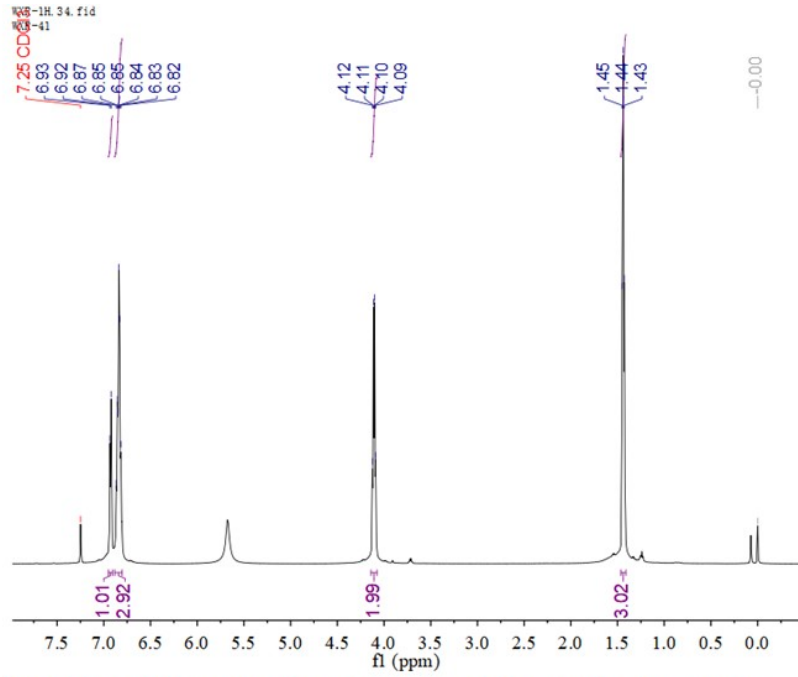
Parameter	Value
1 Origin	Bruker BioSpin GmbH
2 Instrument	spect
3 Solvent	CDCl3
4 Temperature	494.9
5 Pulse Sequence	zg30
6 Experiment	1D
7 Probe	5 mm PABBO BB/ 19F-1H/ D Z-GRD Z114607/0142
8 Number of Scans	16
9 Presaturation Frequency	
10 Acquisition Time	2.7263
11 Acquisition Date	2020-12-03T02:35:00
12 Modification Date	2020-12-03T02:35:00
13 Spectrometer Frequency	600.13
14 Nucleus	1H



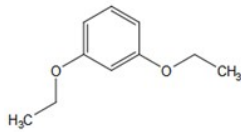
$^1\text{H NMR}$ (600 MHz, Chloroform- d) δ 6.89 (s, 4H), 4.09 (q, $J = 7.0$ Hz, 4H), 1.45 (t, $J = 7.0$ Hz, 6H).



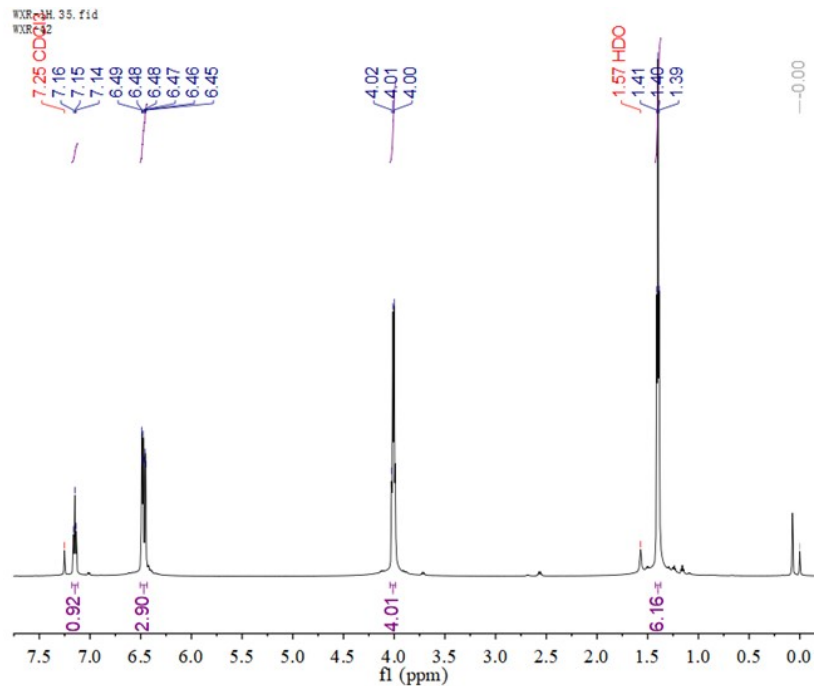
Parameter	Value
1 Origin	Bruker BioSpin GmbH
2 Instrument	spect
3 Solvent	CDCl3
4 Temperature	465.8
5 Pulse Sequence	zg30
6 Experiment	1D
7 Probe	5 mm PABBO BB/ 19F-1H D Z-GRD Z114607 0142
8 Number of Scans	16
9 Presaturation Frequency	
10 Acquisition Time	2.7263
11 Acquisition Date	2020-12-17T11:23:00
12 Modification Date	2020-12-17T11:23:00
13 Spectrometer Frequency	600.13
14 Nucleus	1H



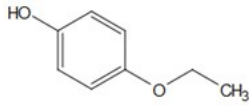
¹H NMR (600 MHz, Chloroform-*d*) δ 6.93 (d, *J* = 7.6 Hz, 1H), 6.88 – 6.80 (m, 3H), 4.11 (q, *J* = 7.0 Hz, 2H), 1.44 (t, *J* = 7.0 Hz, 3H).



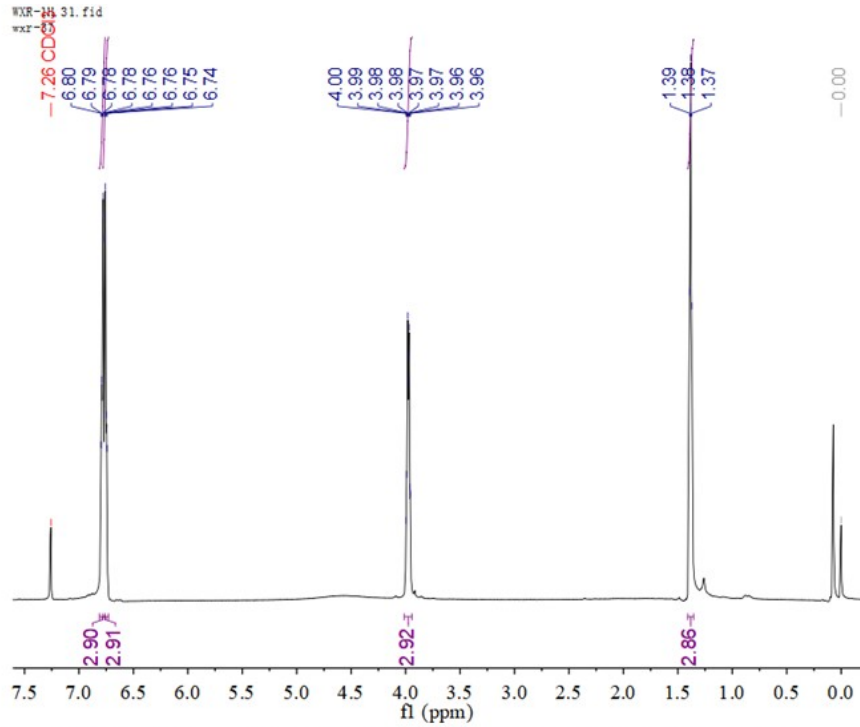
Parameter	Value
1 Origin	Bruker BioSpin GmbH
2 Instrument	spect
3 Solvent	CDCl3
4 Temperature	474.7
5 Pulse Sequence	zg30
6 Experiment	1D
7 Probe	5 mm PABBO BB/ 19F-1H D Z-GRD Z114607 0142
8 Number of Scans	16
9 Presaturation Frequency	
10 Acquisition Time	2.7263
11 Acquisition Date	2020-12-17T11:27:00
12 Modification Date	2020-12-17T11:27:00
13 Spectrometer Frequency	600.13
14 Nucleus	1H



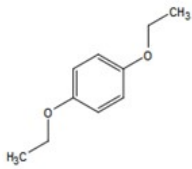
¹H NMR (600 MHz, Chloroform-*d*) δ 7.15 (t, *J* = 8.2 Hz, 1H), 6.50 – 6.44 (m, 3H), 4.01 (q, 4H), 1.40 (t, *J* = 7.0 Hz, 6H).



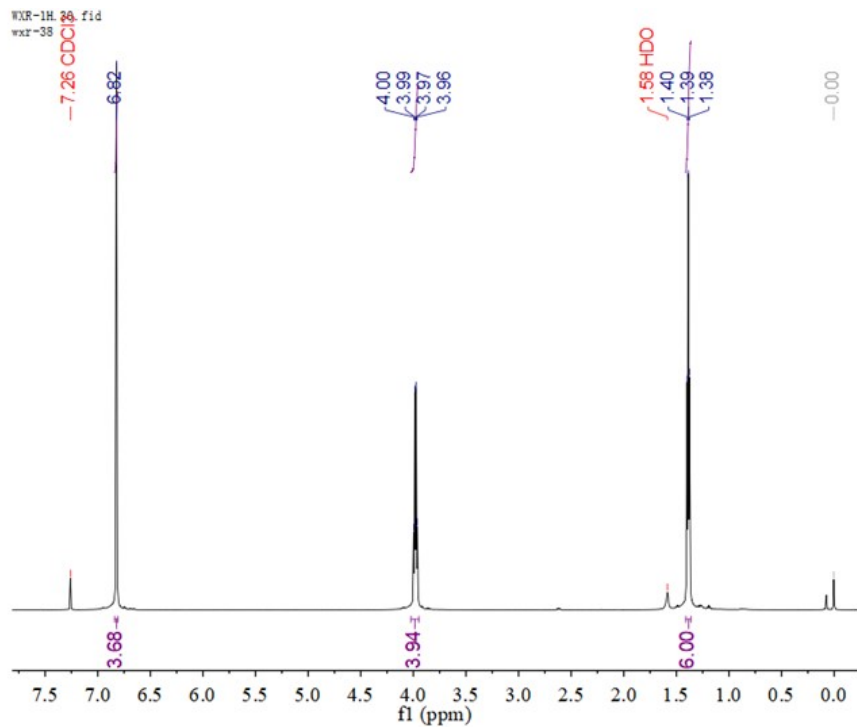
Parameter	Value
1 Origin	Bruker BioSpin GmbH
2 Instrument	spect
3 Solvent	CDCl3
4 Temperature	491.8
5 Pulse Sequence	zg30
6 Experiment	1D
7 Probe	5 mm PABBO BB/ 19F-1H/ D Z-GRD Z114607/ 0142
8 Number of Scans	16
9 Presaturation Frequency	
10 Acquisition Time	2.7263
11 Acquisition Date	2020-12-14T09:08:00
12 Modification Date	2020-12-14T09:08:00
13 Spectrometer Frequency	600.13
14 Nucleus	1H



$^1\text{H NMR}$ (600 MHz, Chloroform-*d*) δ 6.79 (dd, $J = 9.1, 3.3$ Hz, 3H), 6.75 (dd, $J = 9.4, 3.1$ Hz, 3H), 3.98 (q, $J = 7.0, 3.1$ Hz, 3H), 1.38 (t, $J = 7.0$ Hz, 3H).



Parameter	值
1 Origin	Bruker BioSpin GmbH
2 Instrument	spect
3 Solvent	CDCl3
4 Temperature	499.0
5 Pulse Sequence	zg30
6 Experiment	1D
7 Probe	5 mm PABBO BB/ 19F-1H/ D Z-GRD Z114607/ 0142
8 Number of Scans	16
9 Presaturation Frequency	
10 Acquisition Time	2.7263
11 Acquisition Date	2020-12-14T07:56:00
12 Modification Date	2020-12-14T07:56:00
13 Spectrometer Frequency	600.13
14 Nucleus	1H



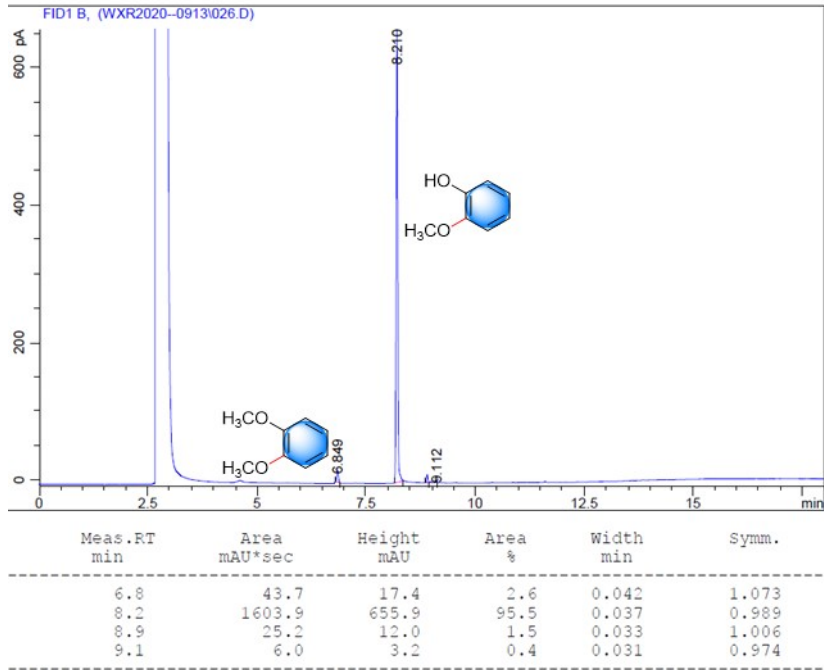
$^1\text{H NMR}$ (600 MHz, Chloroform-*d*) δ 6.82 (s, 4H), 3.98 (q, $J = 7.0$ Hz, 4H), 1.39 (t, $J = 6.9$ Hz, 6H).

7. GC spectra for the alkylations of various diphenols

Data File name: SWU



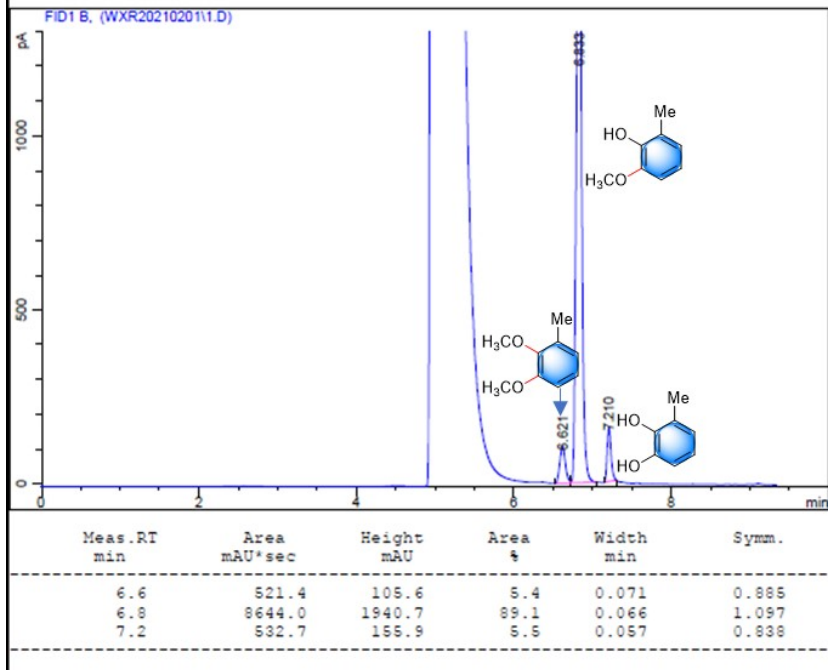
Agilent Technologies



Data File name: SWU



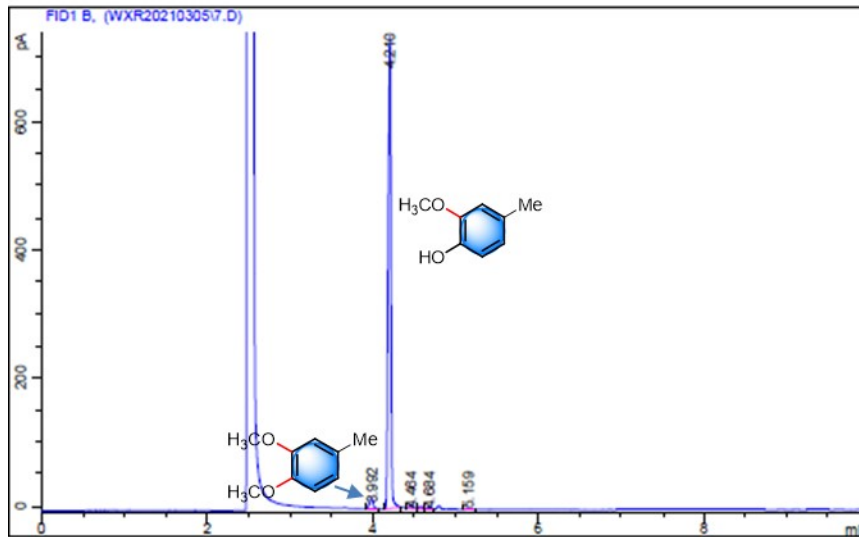
Agilent Technologies



Data File name: SWU



Agilent Technologies

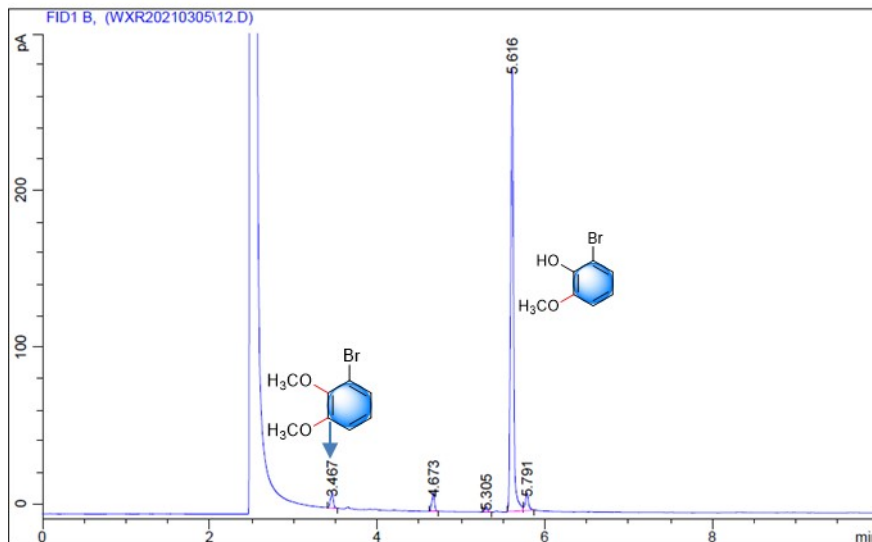


Meas. RT min	Area mAU*sec	Height mAU	Area %	Width min	Symm.
4.0	51.2	15.5	2.7	0.046	1.617
4.2	1759.0	735.4	95.3	0.040	1.467
4.5	16.0	5.0	0.8	0.044	0.714
4.6	8.0	3.3	0.5	0.037	1.212
4.7	7.5	3.3	0.4	0.037	1.151
5.2	5.4	1.8	0.3	0.049	0.915

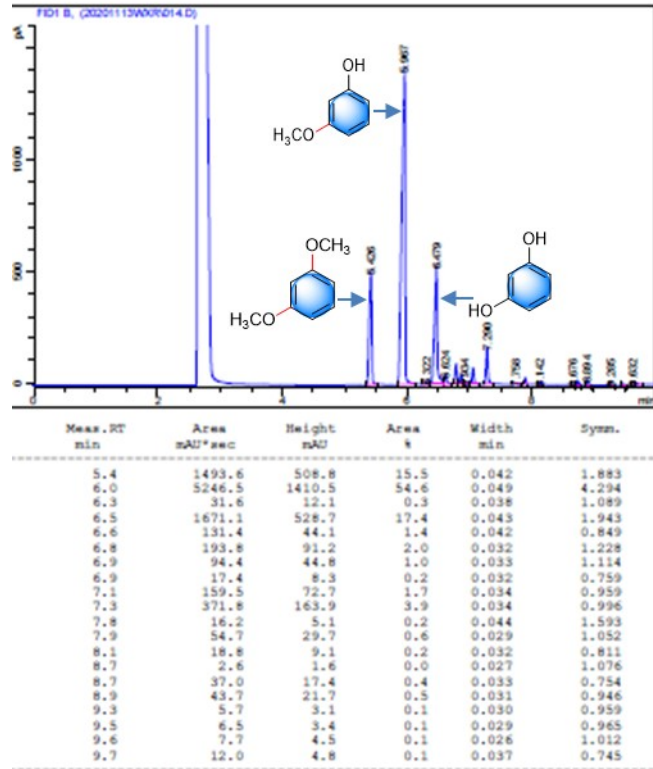
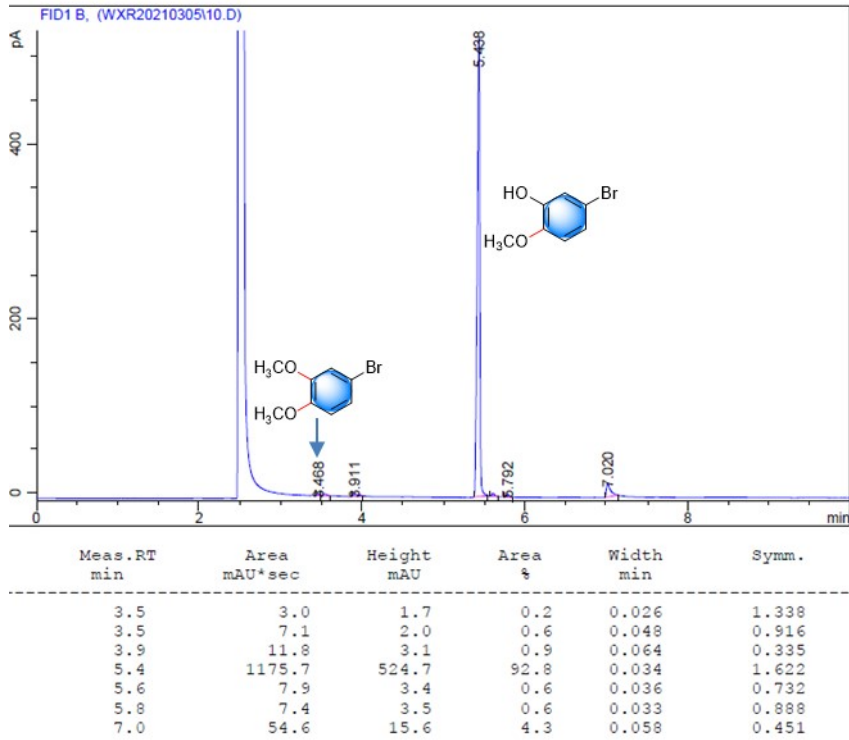
Data File name: SWU



Agilent Technologies

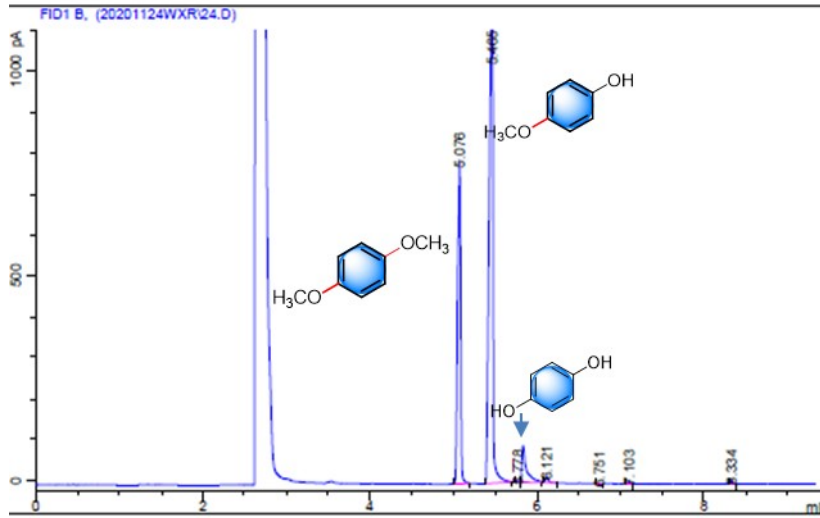


Meas. RT min	Area mAU*sec	Height mAU	Area %	Width min	Symm.
3.5	22.1	9.7	2.9	0.032	1.550
4.7	25.3	11.7	3.3	0.033	1.197
5.3	7.4	3.4	1.0	0.034	1.068
5.6	682.7	281.3	88.8	0.037	1.105
5.8	31.0	11.2	4.0	0.041	0.979





Agilent Technologies

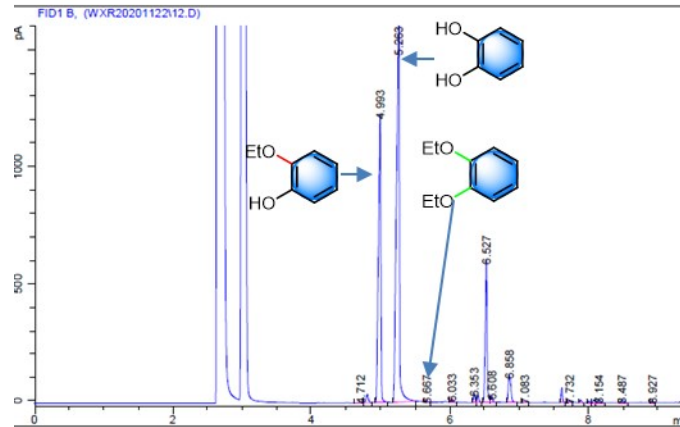


Meas. RT min	Area mAU*sec	Height mAU	Area %	Width min	Symm.
5.1	2022.1	782.9	31.8	0.037	1.864
5.5	3970.3	1364.1	61.9	0.040	2.768
5.8	5.3	2.2	0.1	0.028	1.289
5.8	351.5	89.3	5.5	0.055	0.307
6.1	41.6	15.6	0.6	0.029	1.016
6.8	2.5	1.2	0.0	0.022	0.634
7.1	10.1	3.9	0.2	0.024	0.988
8.3	13.9	5.9	0.2	0.024	0.817

Data File name: SWU



Agilent Technologies

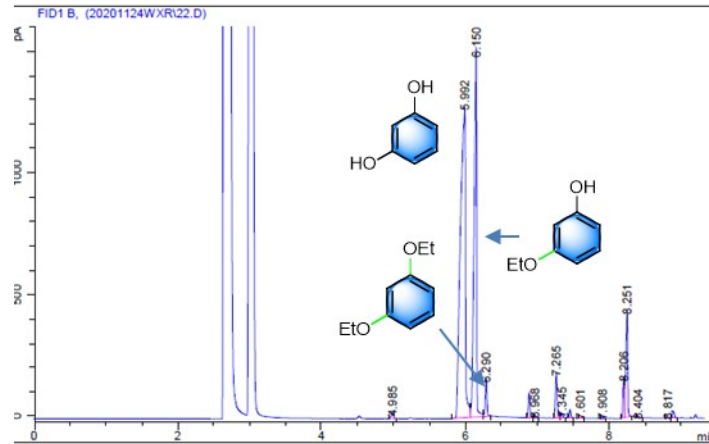


Meas. RT min	Area mAU*sec	Height mAU	Area %	Width min	Symm.
4.7	11.8	3.3	0.1	0.057	1.177
4.8	79.9	23.6	0.8	0.033	1.070
5.0	2950.9	1224.8	23.8	0.035	2.141
5.3	4973.4	1698.0	50.0	0.039	2.733
5.7	13.2	7.9	0.1	0.026	1.139
6.0	29.0	14.9	0.3	0.030	1.110
6.4	64.3	38.5	0.6	0.026	0.990
6.4	54.3	31.2	0.5	0.027	1.056
6.5	1129.1	603.8	11.4	0.028	1.342
6.6	44.1	24.3	0.4	0.027	1.161
6.9	304.0	115.4	3.1	0.036	0.569
7.1	7.2	3.1	0.1	0.034	0.536
7.6	98.5	63.5	1.0	0.024	1.002
7.7	10.8	7.7	0.1	0.022	1.006
7.9	17.2	11.2	0.2	0.024	0.838
8.0	11.6	7.3	0.1	0.025	0.928
8.1	21.2	13.2	0.2	0.025	0.872

Data File name: SWU



Agilent Technologies

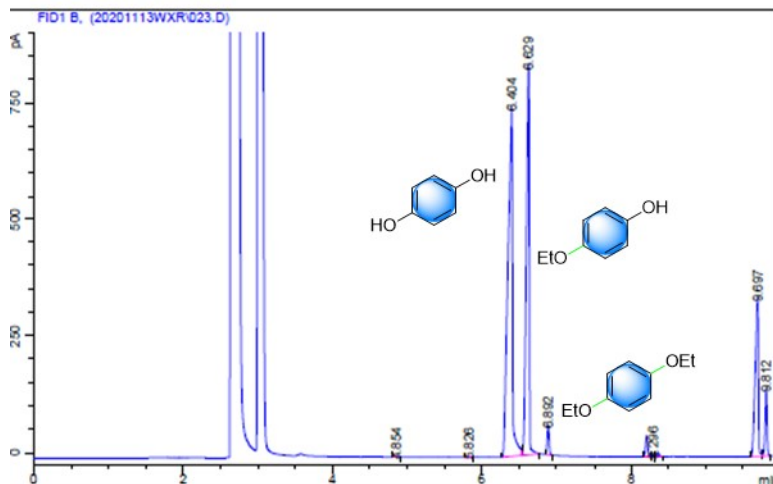


Meas. RT min	Area mAU*sec	Height mAU	Area %	Width min	Symm.
5.0	53.4	24.6	0.4	0.032	1.112
6.0	6231.8	1277.6	51.7	0.061	4.757
6.1	3744.2	1524.4	31.1	0.033	2.939
6.3	251.0	153.5	2.1	0.025	1.142
6.9	169.2	103.1	1.4	0.025	0.930
7.0	21.3	13.4	0.2	0.025	1.027
7.3	339.7	185.9	2.8	0.028	0.822
7.3	34.3	17.9	0.3	0.028	0.907
7.5	54.4	34.3	0.5	0.025	0.997
7.6	2.8	1.7	0.0	0.026	0.753
7.9	11.3	7.0	0.1	0.025	0.962
8.2	236.6	164.0	2.0	0.022	1.497
8.3	836.5	436.6	6.9	0.030	1.894
8.4	8.5	5.0	0.1	0.026	0.544
8.8	3.1	1.7	0.0	0.028	0.729
8.9	56.2	28.5	0.5	0.031	0.665

Data File name: SWU



Agilent Technologies



Meas. RT min	Area mAU*sec	Height mAU	Area %	Width min	Symm.
4.9	5.6	1.9	0.1	0.042	1.037
5.8	5.2	1.0	0.1	0.038	1.137
6.4	3242.3	746.2	48.9	0.059	3.157
6.6	2277.6	891.8	32.3	0.038	2.638
6.9	123.7	63.9	1.8	0.021	1.047
8.2	93.0	44.3	1.3	0.032	0.890
8.3	4.9	2.5	0.1	0.030	0.944
8.4	16.1	8.5	0.2	0.029	0.989
9.7	1012.5	338.0	14.4	0.042	2.751
9.8	274.2	143.9	3.9	0.029	1.223